



Cite this: *Org. Biomol. Chem.*, 2015, **13**, 25

Received 5th August 2014,  
Accepted 10th October 2014

DOI: 10.1039/c4ob01663g

www.rsc.org/obc

# Synthesis of highly functionalized C<sub>60</sub> fullerene derivatives and their applications in material and life sciences

Weibo Yan,<sup>\*a,b</sup> Stefan M. Seifermann,<sup>c</sup> Philippe Pierrat<sup>d</sup> and Stefan Bräse<sup>\*a,e</sup>

Highly functionalized fullerenes can be efficiently constructed by various techniques. However, the challenge is to synthesize highly symmetrical fullerenes. Recently, a number of X-ray structures have been disclosed showing the high symmetry of substituted fullerenes. By reviewing the major types of multi functionalized fullerenes through selected examples with a link to the structural assignments, the authors intend to give a concise overview to the specialist in the field and to provide the non-specialist with a tool box of possibilities.

## 1. Introduction

Carbon rich nanostructures have been a major topic in chemical research over the past four decades.<sup>1–6</sup> In particular, fullerenes that combine three-dimensionality with unique photoelectric and electrochemical properties are extremely promising nanostructures for the preparation of new advanced materials<sup>7,8</sup> and biologically active molecules.<sup>9–12</sup>

At present, the most widely used commercial fullerene derivative is a mono-functional [6,6]-phenyl-C<sub>61</sub>-butyric acid methyl ester (PCBM). It is one of the most important electron acceptor materials presently used in organic bulk-heterojunction solar cells.<sup>13</sup>

<sup>a</sup>Institute of Organic Chemistry, KIT-Campus South, Fritz-Haber Weg 6, 76131 Karlsruhe, Germany. E-mail: braese@kit.edu; Fax: (+49) 721-608-48581; Tel: (+49) 721-608-42902

<sup>b</sup>Beijing National Laboratory for Molecular Sciences, State Key Laboratory of Rare Earth Materials Chemistry and Applications, College of Chemistry and Molecular Engineering, Peking University, China

<sup>c</sup>CYNORA GmbH, Bruchsal, Germany

<sup>d</sup>Laboratoire de Conception et Application de Molécules Bioactives CNRS – Université de Strasbourg, Faculté de Pharmacie, 74 route du Rhin 67401 Illkirch, France

<sup>e</sup>Institute of Toxicology and Genetics, KIT, Campus North, Hermann-von-Helmholtz-Platz 1, 76344 Eggenstein-Leopoldshafen, Germany



Weibo Yan

Weibo Yan started studying organic chemistry and organic functional materials at the Nankai University in Tianjin, China, in 2006 and obtained his PhD in organic chemistry from the institute of elemento-organic chemistry in 2011. After that, he worked as a postdoctoral fellow in organic nanostructures at Karlsruhe Institute of Technology (KIT) in Germany from 2011 to 2012. Since January 2013, Weibo worked as a postdoctoral fellow

at the Institute of Inorganic Chemistry, College of Chemistry and Molecular Engineering, Peking University in Beijing on the synthesis of OLED, solar cell materials and the fabrication of their devices.



Stefan M. Seifermann

Stefan Seifermann studied chemistry at Karlsruhe Institute of Technology (KIT). He worked in the group of Stefan Bräse as a member of the Center for Functional Nanostructures (CFN) in the field of fullerene chemistry. After receiving his PhD in 2013, he joined CYNORA GmbH in Bruchsal, Germany, where he is currently studying the development of new materials for Organic Light Emitting Devices (OLEDs).



Hexakis-substituted  $C_{60}$  adducts with a  $T_h$ -symmetrical octahedral addition pattern are unique organic molecules with an appealing compact spherical scaffold for the construction of multifunctional nanomaterials. In addition, many bis-, tris-, tetrakis- and pentakis-functionalized  $C_{60}$  derivatives with special electronic and structural properties have been investigated. They are potentially useful for applications in 2D/3D metal-organic frameworks,<sup>14</sup> sensitizers for photodynamic therapy,<sup>15</sup> solar energy conversion<sup>13</sup> as photoactive molecular devices,<sup>16</sup> liquid crystals materials,<sup>17</sup> thermoresponsive materials,<sup>18</sup>  $C_{60}$ -polymer hybrid materials,<sup>19</sup> or inhibitors of bacterial growth,<sup>10</sup> and so on.

In the last two decades, well-optimized and widely used synthetic methods such as the Bingel cyclopropanation,<sup>20</sup> 1,3-dipolar additions,<sup>21,22</sup> and Diels-Alder reactions,<sup>23–28</sup> provided readily accessible building blocks for higher molecular architectures and optoelectronic devices. Several groups have provided in-depth insights into the fascinating field of functionalized fullerenes.

Thus, in this non-comprehensive review, new synthetic strategies of more higher-functionalized fullerene derivatives are summarized. Their properties, application or potential application value will be briefly described and discussed.

The addition of atoms (H, F, Cl, Br, O) to the fullerene core or the addition of radicals as long as they are not stereoselective are not presented in this overview.

### 1.1. Stereochemical considerations

The addition of functional groups to the  $C_{60}$ -fullerene core leads to various substitution patterns.<sup>1</sup> In most cases, the

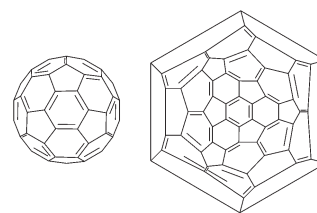


Fig. 1 Fullerene  $C_{60}$  and its Schlegel diagram.

Table 1 Examples for substitution patterns of fullerenes

Substitution	Symmetry	Space-group
Bis	$I_h$ , <sup>13</sup> $C_{1v}$ , $C_{2v}$ , $C_s$ <sup>30</sup>	$P\bar{1}$ <sup>31</sup>
Tris	$C_{2v}$ , <sup>16</sup> $C_{2v}$ <sup>30</sup>	
Tetrakis	$D_{2h}$ , <sup>30</sup> $C_{2v}$ <sup>30</sup>	$P\bar{1}$ <sup>32</sup>
Pentakis	$C_{2v}$ , <sup>33</sup> $C_s$ , <sup>30</sup> $C_s$ , <sup>34</sup> $C_{5v}$ <sup>34</sup>	
Hexakis	$D_{2h}$ , <sup>35</sup> $T_h$ , <sup>36</sup> $T$ <sup>37</sup>	$C2$ <sup>38</sup>
Decakis	$D_{5h}$ <sup>39</sup>	

electrophilic and reactive [6,6]-bonds (Fig. 1, bold) are the starting points.

Besides regiochemical issues, stereochemistry plays an important role as well.<sup>1</sup> While monosubstituted fullerenes without chiral substituents are in principal achiral, most of the higher substituted fullerenes exhibit – depending on their substitution pattern – chirality.<sup>1</sup> As these issues have been discussed in excellent reviews, we will just give a short overview.

Starting from fullerene with  $I_h$  symmetry, a number of other symmetric entities can be derived:<sup>29</sup>  $C_1$ ,  $C_s$ ,  $C_2$ ,  $C_{2v}$ ,  $C_{2h}$ ,  $C_{3v}$ ,  $C_{3h}$ ,  $D_2$ ,  $D_3$ ,  $D_5$ ,  $D_{2h}$ ,  $D_{6h}$ ,  $D_{2d}$ ,  $D_{5d}$ ,  $S_4$ ,  $I_h$ ,  $T_h$ ,  $T$ . However, not all of them have been observed experimentally (Table 1).



Philippe Pierrat

Philippe Pierrat studied chemistry at Nancy University in France. After 3 years of research in the field of organometallic chemistry in the lab headed by Pr. Yves Fort, he obtained his PhD in 2006. Next, he joined the research group of Pr. Stefan Bräse with an Alexander von Humboldt post-doctoral fellowship to work on fullerene chemistry. In 2009, he was appointed assistant Professor of Organic chemistry at the Strasbourg University in the research group of Dr Luc Lebeau, where he is currently developing new bio-responsive cationic vectors for gene delivery applications.



Stefan Bräse

Stefan Bräse studied in Göttingen (Germany), Bangor (UK) and Marseille (France) and received his Ph.D. in 1995, after working with Armin de Meijere in Göttingen. After post-doctoral appointments at Uppsala University (Jan E. Bäckvall) and The Scripps Research Institute (K. C. Nicolaou), he began his independent research career at the RWTH Aachen in 1997 (associated to Dieter Enders). In 2001, he finished his habilitation and moved to the University of Bonn as professor for organic chemistry. Since 2003, he is full professor at the Karlsruhe Institute of Technology and since 2012 director of the Institute of Toxicology and Genetics at the KIT. His research interests include methods in drug discovery (including drug-delivery), combinatorial chemistry towards the synthesis of biologically active compounds, total synthesis of natural products and nanotechnology.



## 2. Multiple functionalized fullerenes

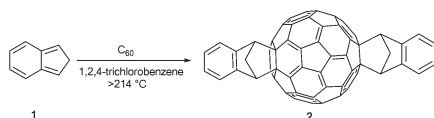
### 2.1. Bis-functional fullerenes

Most of the functionalized fullerenes known to date are di-substituted derivatives because they are promising materials for optoelectronic devices and are easily accessible by a variety of synthetic protocols.

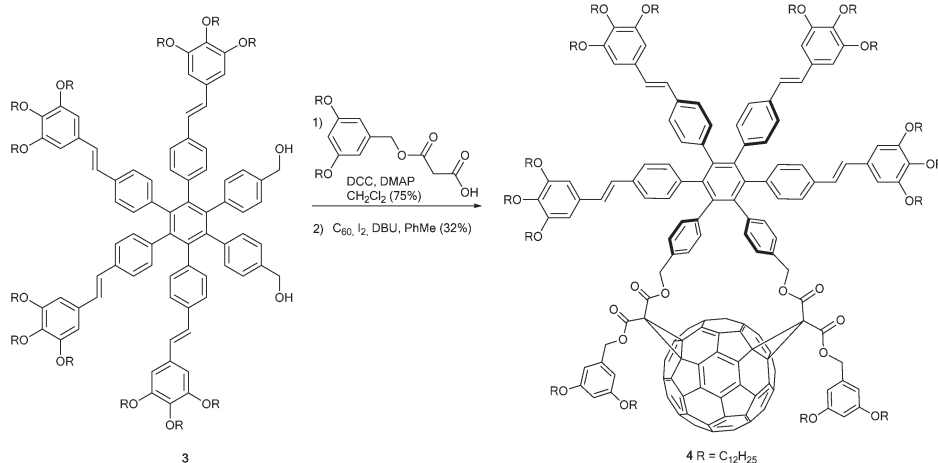
In that context *e.g.* He *et al.* synthesized ICBA (**2**) (indene- $C_{60}$ -bis-adduct) by using a simple one-pot reaction.<sup>13</sup> Starting from indene (**1**) and  $C_{60}$  in 1,2,4-trichlorobenzene as the solvent they obtained ICBA (**2**) in 34% yield (Scheme 1). This bis-adduct exhibits stronger absorption of visible light (400–800 nm) and a 0.17 eV higher LUMO energy level than PCBM, together with an improved solubility in common organic solvents (higher than 90 mg mL<sup>-1</sup> in chloroform).

Furthermore, compared to P3HT/bisPCBM devices, PSCs based on the P3HT/ICBA system show better performance (4.5% *vs.* 5.4% PCE). Thus, ICBA is a promising candidate to be used as acceptor material in high performance PSCs.

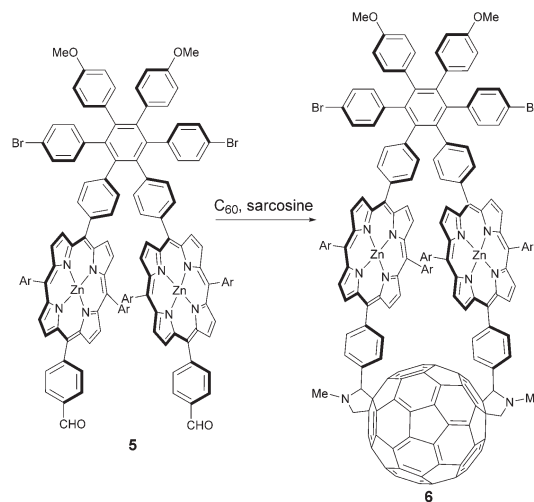
A multiphoton absorbing fullerene derivative was published by Figueira-Duarte *et al.*<sup>15</sup> They reported fullerene bis-adduct **4** bearing a hexaphenyl benzene based MPA (multi photon absorption) dye **3**, connected to  $C_{60}$  *via* two malonate units. Its synthesis was carried out in a Bingel cyclopropanation of the corresponding bis-malonate with  $C_{60}$ , I<sub>2</sub>, and 1,8-diazabicyclo [5.4.0]undec-7-ene (DBU) in toluene at room temperature in 32% yield (Scheme 2). The authors found that the star-shaped system with increased dimensionality and branched structures, lead to the highly effective multiphoton absorption of compound **4**.



Scheme 1 Synthetic route to ICBA (indene- $C_{60}$  bis-adduct).



Scheme 2 Synthetic route to a bis-functional fullerene with star-shaped chromophore.

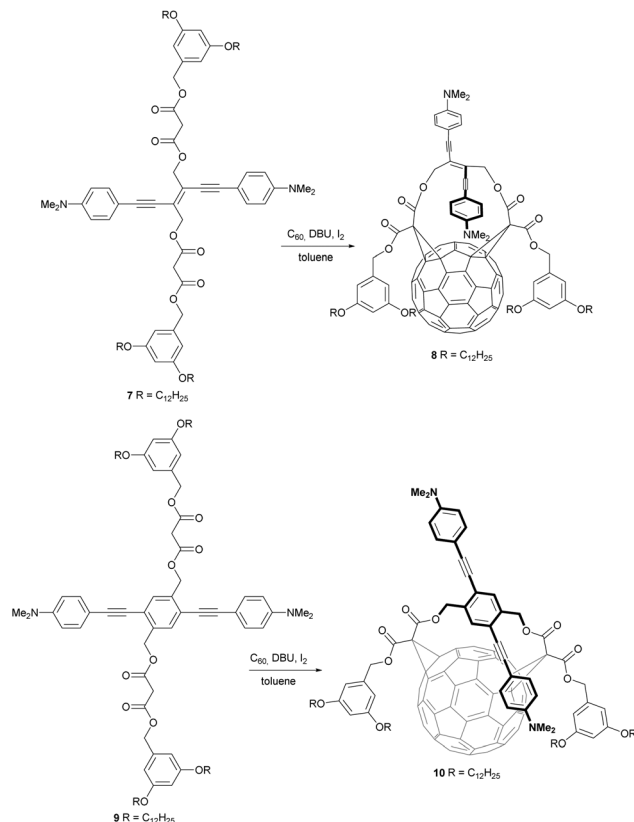


Scheme 3 Synthesis of a macrocyclic diporphyrin-fullerene with  $C_2$  symmetry and *trans*-2 disubstitution pattern.

The authors showed that fluorescence of the  $\pi$ -conjugated system was quenched by the fullerene core due to singlet-singlet energy transfer to the fullerene fragment, followed by intersystem crossing to generate a fullerene-centered triplet. Therefore, in  $C_{60}$ -MPA dye dyads the optical limiting properties of  $C_{60}$  are improved which makes such compounds interesting candidates for the protection of optical devices. Furthermore, an application in photodynamic therapy could be possible.

Garg *et al.* prepared a macrocyclic diporphyrin-fullerene triad **6** that could be used as an artificial photosynthetic reaction centre.<sup>16</sup> That compound was synthesized in 20% yield *via* an unusual double 1,3-dipolar cycloaddition of  $C_{60}$  with the azomethine ylides formed from *N*-methylglycine (sarcosine) and a hexaphenylbenzene derivative bearing two aldehyde functionalized porphyrin units **5** (Scheme 3). The hexaphenylbenzene architecture was used to establish the required rigidity of the macrocyclic diporphyrin-fullerene. Thus, enforced by the strained 42-atom macrocycle, *trans*-2



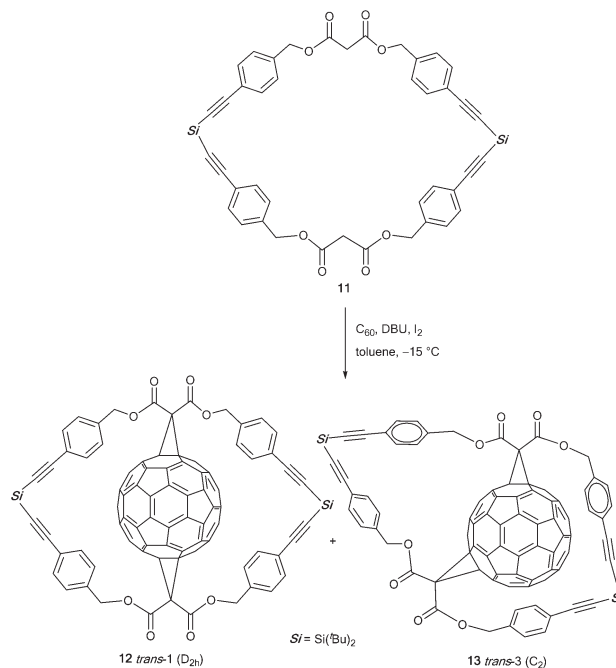


**Scheme 4** Synthesis of bis-adducts with  $\pi$ -conjugated substituents.

disubstitution pattern and therefore  $C_2$ -symmetry of the resulting fullerene derivative were achieved. The rigidity of this system results in a very fast photoinduced electron transfer (2000 times faster than charge recombination) and a relatively long-lived charge separated state. In addition, compared to corresponding compounds bearing only one porphyrin unit per fullerene core, the absorption cross section for photoinduced electron transfer is doubled, which leads to a high quantum yield of charge separation. Furthermore the hexaphenylbenzene unit allows for additional functionalization such as with antenna moieties. This way an antenna-reaction centre complex can be obtained.

Besides the above mentioned charge transfers between  $C_{60}$  and its substituents, there can also be  $\pi$ - $\pi$  interactions. In this context Figueira-Duarte *et al.* presented fullerene bis-adducts **8** and **10** that consist of a  $\pi$ -conjugated oligomer unit showing  $\pi$ - $\pi$  interaction with the  $C_{60}$  core (Scheme 4).<sup>40</sup> Compounds **8** and **10** were synthesized from  $C_{60}$  and the corresponding bis-malonates **7** and **8**, respectively, under the previously mentioned reaction conditions developed by Diederich. The yields were 19% for the *cis*-2-bis-adduct **8** and 38% for the *trans*-4-bis-adduct **10**.

Due to ring strain effects in these two macrocyclic dyads, the fullerene moiety and the  $\pi$ -conjugated oligomer substituent come into van der Waals contact. Thus,  $\pi$ - $\pi$  interactions between these conjugated systems are enabled. The authors proved these  $\pi$ - $\pi$  interactions by a significant red-shift in the



**Scheme 5** Synthetic route to new fullerene building blocks.

UV/VIS spectra of compounds **8** (24 nm) and **10** (34 nm), as compared to their non-fullerene-bound analogues. They assigned this effect to the lowering of the oligomers' HOMO–LUMO gaps by through-space interactions with the electron withdrawing  $C_{60}$  core. These intramolecular interactions have a significant influence on the electronic coupling of the two aniline redox units in the dyad.

The above mentioned fullerene bis-adducts all have high potential for applications, due to their electronic and optoelectronic properties. Additionally, multiple functionalized fullerenes are well-suited as building blocks for nanomaterials due to their structural variety.

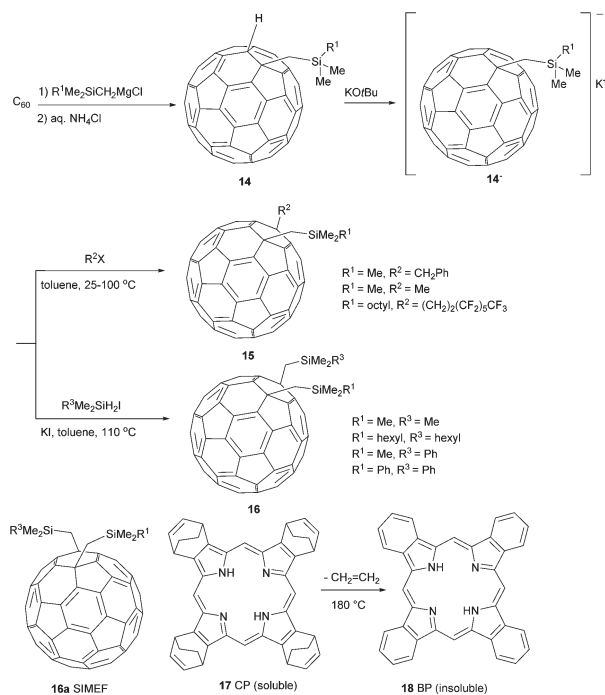
Sigwalt *et al.* reported the synthesis of two fullerene bis-adducts (**12**, **13**) that can be used as precursors for nanomaterials (Scheme 5).<sup>41</sup> By reacting  $C_{60}$  with cyclic bis-malonate **11** in a modified version of a procedure by Nierengarten *et al.*<sup>42</sup> they obtained compounds **12** and **13** in 8% and 18% yield, respectively.<sup>42</sup> The authors assigned the excellent stereo-selectivity of this reaction (no further isomers were obtained) to both the ring size of cyclic bis-malonate **11** and the minimum ring strain in *trans*-1 bis-adduct **12** and *trans*-3 bis-adduct **13**. The former can especially serve as a highly potent building block. Further functionalization of this compound can give access to *all-e*-tetrakis-adducts carrying four substituents around the equator belt of their  $C_{60}$  core. Such structures can provide a variety of unprecedented nanostructures.

Matsuo *et al.* reported a protocol that gives improved yields in mono-addition reactions of Grignard reagents onto Buckminsterfullerenes.

They found out that the addition of DMF as a polar solvent enhanced the reactions of tri(organo)silylmethylmagnesium chlorides with fullerenes to excellent yields within 5–15 min

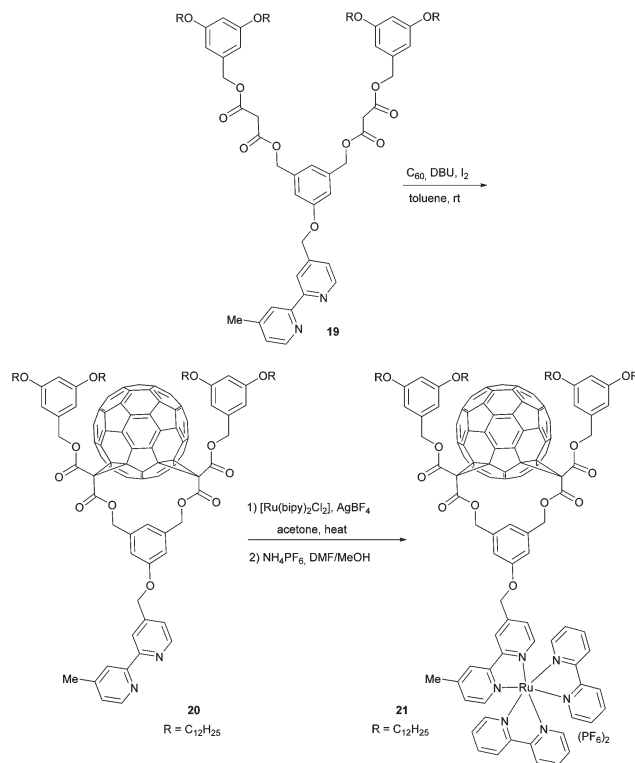




Scheme 6 Synthetic route to 1,4-bis-functional fullerenes.<sup>44</sup>

(Scheme 6).<sup>43</sup> Furthermore, the authors established a protocol that allows for regioselective alkylation of the corresponding anions **14** and gives rise to 1,4-di(organo)[60]fullerenes **15** in up to 93% yield. Cyclic voltammetry measurements revealed that almost all of the compounds they synthesized had three reversible reduction states around 1.03 V, 1.65 V, 2.27 V and calculated LUMO levels of about 3.77 eV. As these values are slightly higher than those of PCBM (LUMO: 3.80 eV), 1,4-di(organo)fullerenes are interesting alternatives to PCBM. In addition, the authors were able to tune the bulk properties and solubility of these materials by varying the chain length of the organic rests  $R^1$  and  $R^2$ .

In a second publication, Matsuo *et al.* took advantage of this structure/morphology relationship for the construction of solution-processed bulk heterojunction (BHJ) solar cells with p-i-n structures.<sup>44</sup> Their strategy was to spin coat a 3:7 mixture of the donor CP (**17**) and the acceptor (**16a**) in a chloroform–chlorobenzene solution as the i layer. Upon thermal annealing at 180 °C, an interdigitated bulk heterojunction was generated due to a thermal retro-Diels–Alder reaction of **17** to insoluble, crystalline BP (**18**), and due to crystallization of SIMEF **16a** (transition amorphous crystalline at 149 °C). SEM images clearly revealed a column/canyon structure of crystalline BP in the device. Since such structures were not found in PCBM-based devices (crystallization of PCBM at 195 °C), the authors ascribe this effect to SIMEF **16a**, which crystallizes at 149 °C and therefore forms a crystallization matrix, forcing BP (**18**) to build columnar crystals. Furthermore, with a PCE of 5.2%, the BP/SIMEF-based OPV cell was one of the most efficient reported in the literature (2009). Therefore, SIMEF derivatives are promising candidates both as

Scheme 7 Amphiphilic  $C_{60}$ –Ru(bipy)<sub>3</sub> hybrid material.

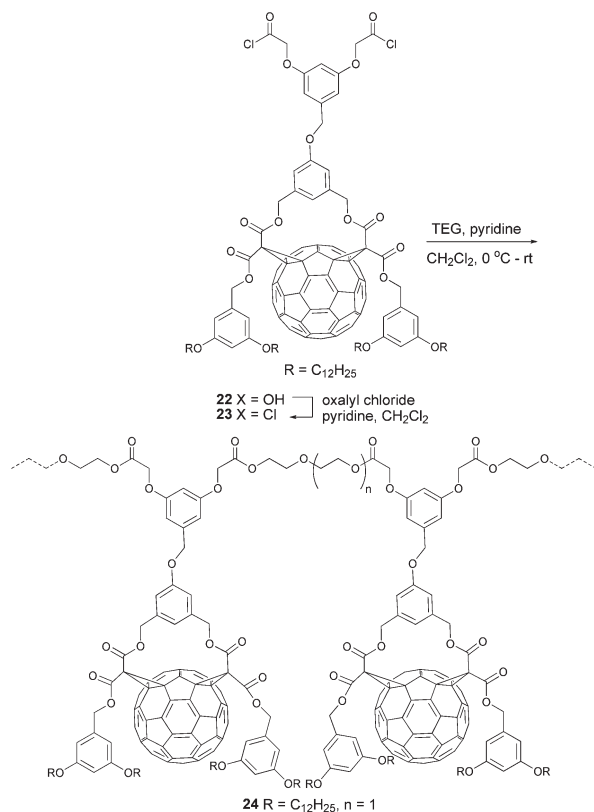
acceptor and morphology determining materials for BHJ solar cells.

In terms of fullerene derivatives, the Nierengarten group contributed another interesting publication, describing good film-forming properties for OPV applications.<sup>45</sup> They prepared  $C_{60}$ –Ru(II) hybrid structure **21** in 14% yield by first reacting the fullerene with 2,2'-bipyridine containing bis-malonate **19** with compound **20**, followed by complexation with  $[Ru(bipy)_2Cl_2]$  (Scheme 7). Due to its amphiphilic character and the alkyl chain decorated bis-malonate moiety, which prevents aggregation of the fullerene subunits, compound **21** forms stable Langmuir films. These films show reversible behaviour in successive compression expansion cycles. In addition the authors proved the occurrence of a photoinduced electron transfer from the Ru(bipy)<sub>2</sub> unit to the fullerene core due to effective quenching of the Ru(bipy)<sub>2</sub> MLCT emission by the latter. The aforementioned properties turns amphiphilic  $C_{60}$ –Ru(bipy)<sub>2</sub> derivatives into very promising candidates for the use in solution processed OPVs.

A different method towards fullerenes with good film-forming properties was presented by Nava *et al.*<sup>19</sup> They prepared a fullerene-containing polymer **24** through polycondensation of acyl chloride **23**, which was synthesized from carboxylic acid **22** and tetraethyleneglycol in 70% yield (Scheme 8).

Because polyester **24** has good solubility in common organic solvents and good film-forming properties, combined with the electronic properties of  $C_{60}$ , it was used in all-polymer donor/acceptor BHJ photovoltaic cells. Although the latter





**Scheme 8** Synthetic route to fullerene-based polyesters.<sup>19</sup>

showed low short circuit currents and low open circuit voltages compared to optimized PCBM-based devices, polymers like **24** remain interesting candidates for OPV applications.

In contrast to the aforementioned covalent fullerene-containing polymer, fullero-dendrimers represent a class of monodisperse macromolecular fullerene derivatives, based on non-covalent interactions.<sup>46–48</sup> In this context van de Coevering *et al.* reported a non-covalent octa-fullero-dendrimer **27**.<sup>49</sup> This compound bears a central anionic tetra[bis(benzoylammonium)aryl]silane unit that interacts with eight anionic fullerene bis-adducts. Its synthesis was carried out by an anion exchange reaction between octa-ammonium salt **26** and 8 equiv. of Na[C<sub>60</sub>CO<sub>2</sub>] (**25**) (Scheme 9). The authors claim that in photoluminescence experiments, the characteristic emission of the dendritic benzyl ether units was fully quenched upon excitation in the UV region. This indicates an intramolecular energy transfer from the lowest dendrite singlet excited state of the dendritic core to the peripheral fullerene singlet excited state. Thus, this kind of core-shell fullerene dendrimers may lead to the preparation of unprecedented photoactive molecular devices like antennas for light-harvesting or fullero-dendrimer-based organic solar cells.

Besides the non-covalent dendrimeric structure **27**, fullero-dendrimers based on covalent bonds are known as well. Hahn *et al.*, for instance, reported three generations (G<sub>n</sub>) of fullero-dendrimers **30** bearing a central hexaphenyl benzene core and six (compound **30a**), 12 (**30b**) or 24 (**30c**) peripheral C<sub>60</sub>

units.<sup>50</sup> These structures were synthesized starting from dialcohol **28** and first esterified to give bis-(aryl)alkynes **28a–c**. The key step was a cobalt-catalyzed cyclotrimerization of the alkynes to yield the corresponding n-generation dendrimers **30a–c** in 93%, 62% and 24% yield, respectively. For clarity, in Fig. 2 the full structure of compound **30b** is depicted separately (Scheme 10).

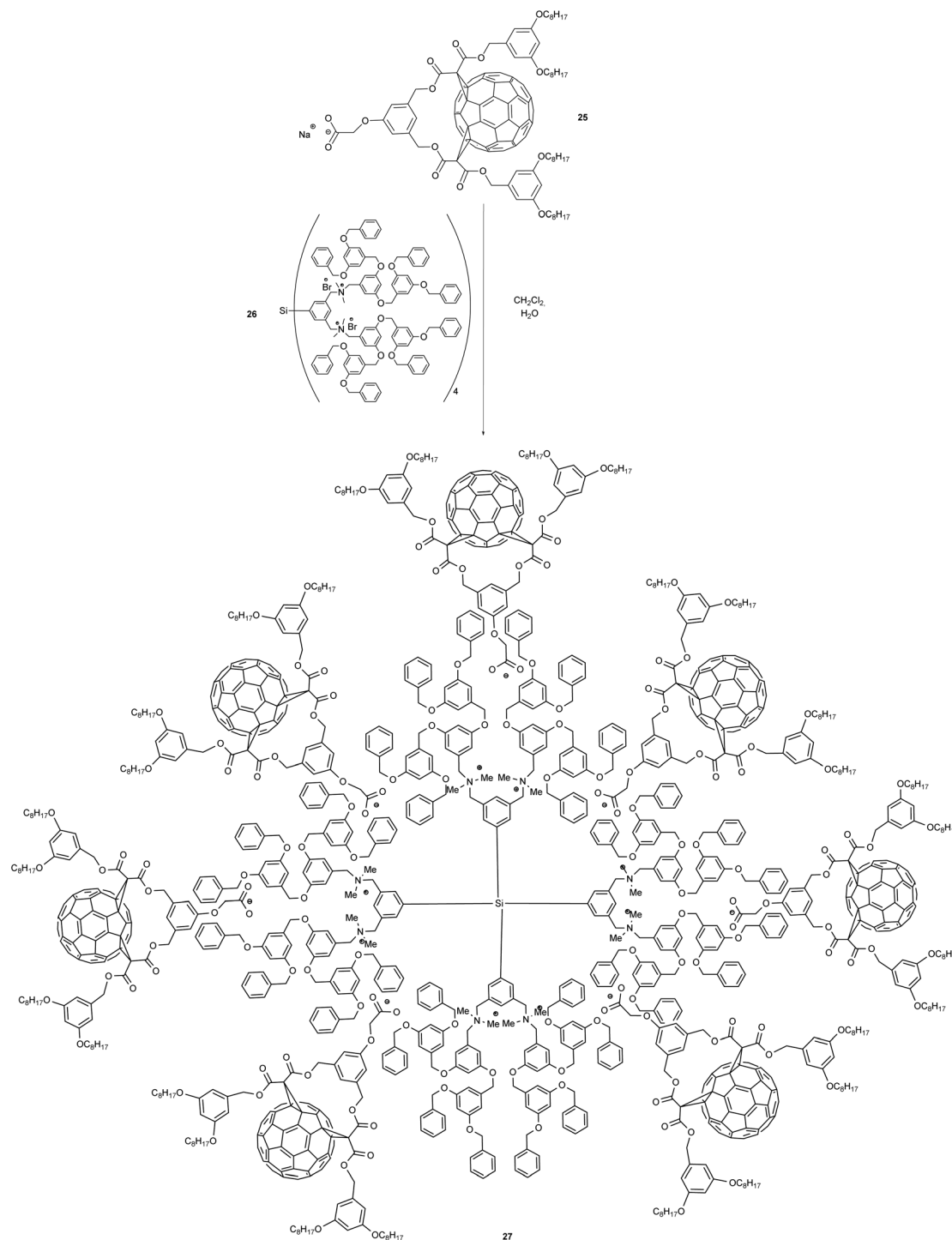
## 2.2. Tris-functionalized fullerenes

The addition of symmetric malonate units onto C<sub>60</sub> can theoretically give 14 different regioisomers. Hirsch *et al.* discovered that the *all-equatorial e,e,e*-isomers could be synthesized selectively under specific reaction conditions, explaining why the *e,e,e*-isomers are the most prominent members in the family of trisubstituted fullerenes.<sup>51</sup> In this context, Sigwalt *et al.*<sup>52</sup> reported an expeditious synthesis of fullerene *e,e,e*-tris adducts through a threefold Bingel reaction between C<sub>60</sub> and *t*-butyl-(trialkoxysilane)-based tris-malonates **31a–c** (Scheme 11). Cyclopropanation of C<sub>60</sub> with these malonates in the presence of I<sub>2</sub> and DBU in toluene at –15 °C gave **32a–c** with 8%, 26% and 14% yield, respectively. In this case, the silane moiety acts as a tether that forces the three adjacent malonate units into the *e,e,e*-addition pattern. After treatment of **32a** with HF-pyridine in THF or **32b** and **32c** with BF<sub>3</sub>·Et<sub>2</sub>O in CH<sub>2</sub>Cl<sub>2</sub>–CH<sub>3</sub>CN, the tether was removed to give triols **33a–c** in 85%, 99% and 67% yield, respectively. Bearing three free hydroxyl groups, the latter can serve as precious building blocks for a plenty of further chemical transformations. In addition, their *e,e,e*-fullerene addition pattern makes them perfectly suited as precursors for fullerene hexakis-adducts with an octahedral addition pattern.<sup>53</sup>

This efficient method for the preparation of optically pure *e,e,e*-tris-adducts was further developed by Nierengarten *et al.* (Scheme 12).<sup>54</sup> They used Si-tethered tris(malonate) **34**, bearing enantiomerically pure dioxolane dimethanol entities, to get two diastereomers **35a** (7%) and **35b** (5%), evoked by the inherently chiral addition pattern on the fullerene core. The structure of one of the diastereomers was elucidated using X-ray crystal structure analysis allowing also therefore the stereochemistry of the other one. The final hydrolysis of the malonate moieties gave access to optically pure C<sub>60</sub>-tris-(malonic acid) derivatives **36a** and **36b** in 77% and 87% yield, respectively.

Besides tris-additions by threefold Bingel reactions, combinations of Bingel reactions and Diels–Alder [4 + 2]-cycloadditions are widely used to synthesize fullerene-tris-adducts. In this respect, the group of Diederich reported *e,e-trans*-1-tris-adduct **38**, which was prepared from C<sub>60</sub> and bis(1,3-butadienyl)malonate derivative **37** in a successive nucleophilic cyclopropanation-[4 + 2]-cycloaddition sequence (Scheme 13).<sup>55,56</sup> The reaction proceeded diastereoselectively in 60% yield. Furthermore, the authors demonstrated the high synthetic potential of compound **38** as a building block by regioselective conversion into tetrakis-, pentakis-, and hexakis-adducts (structures not shown).





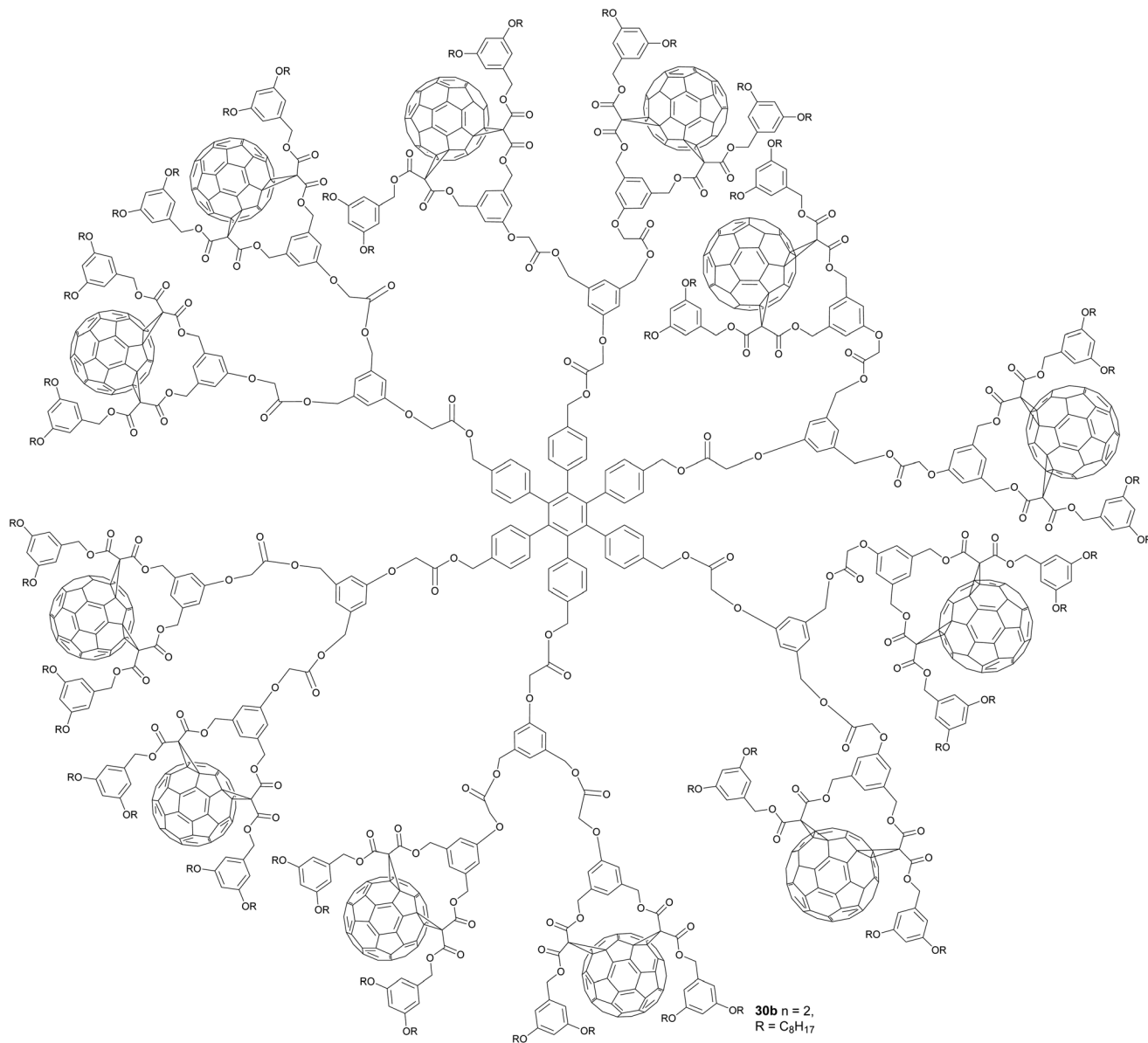
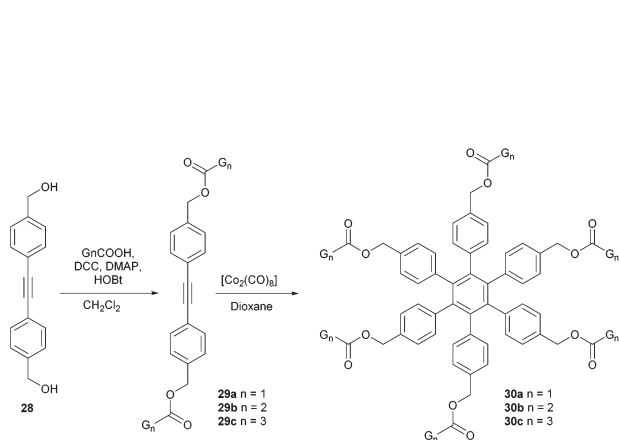
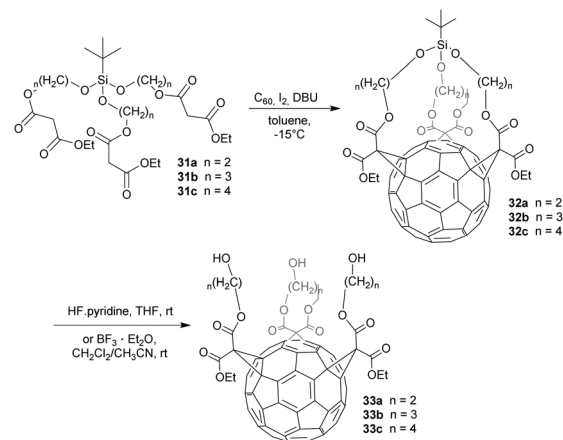
**Scheme 9** Synthesis of a self-assembled octa-fullero-dendrimer.

A tether-based synthetic route towards *cis*-2,*cis*-2,*trans*-3, tris-adducts was published by Nierengarten *et al.* By treatment of mono-functional fullerene **39**, which had been prepared from the corresponding THP-protected diol after deprotection and reaction with ethyl malonyl chloride (conditions not shown), with DBU and  $I_2$  in toluene under high dilution conditions, fullerene **40** was synthesized in 32% yield (Scheme 14).<sup>56,57</sup>

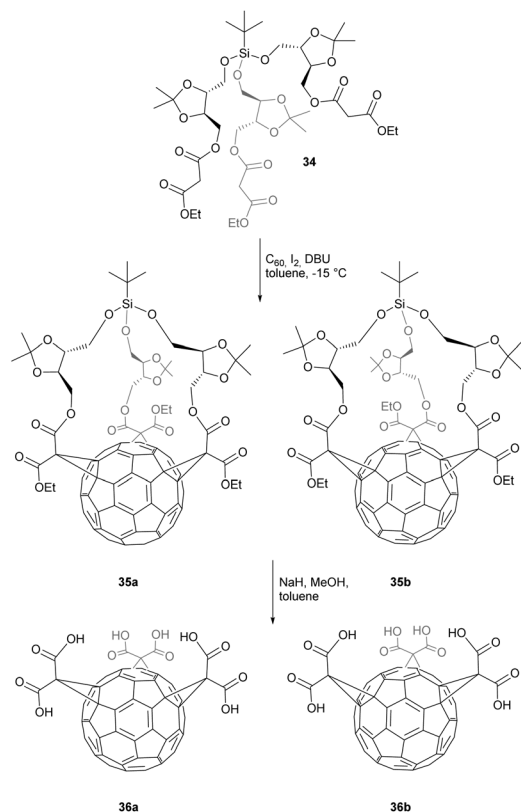
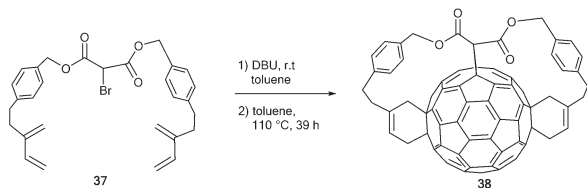
The addition pattern, which is caused by the *m*-xylene units connecting the three malonate units, was proven by NMR spectroscopy.

All of the aforementioned regioselective syntheses of fullerene tris-adducts are based on tethers that force the substituents into the desired positions with their structure or length.

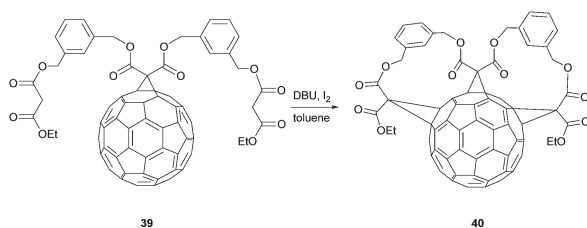


Fig. 2 Structure of 2nd-generation dendrimer **30b**.Scheme 10 Synthesis of fullero-dendrimers **30a–c**.Scheme 11  $C_{60}$ -e,e,e-tris-adducts bearing free hydroxy groups.



Scheme 12 Optically pure C<sub>60</sub>-e,e,e-tris(malonic acids).

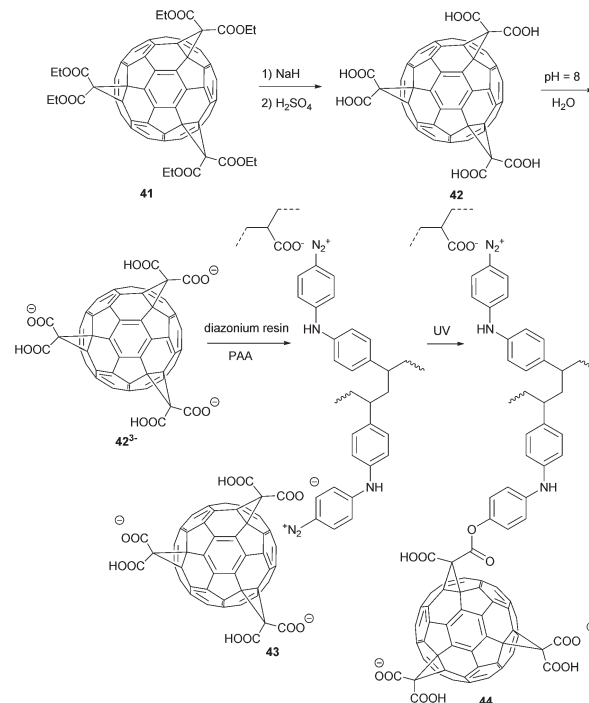
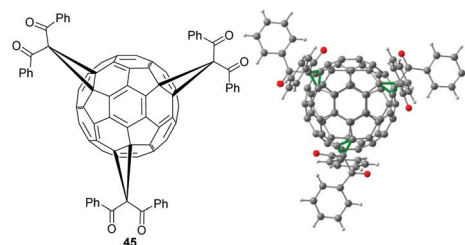
Scheme 13 Tethered synthesis of an e,e,trans-1-tris-adduct.



Scheme 14 Synthesis of a cis-2, cis-2, trans-3-tris-adduct.

Regardless of that, the Hirsch group discovered that successive additions of malonate derivatives onto C<sub>60</sub> proceeded with remarkably high regioselectivity.<sup>51,58,59</sup> They took advantage of this regioselectivity in order to synthesize C<sub>60</sub>-tris-malonic acid **42** from tris(diethylmalonate) derivative **41** (Scheme 15).<sup>60</sup>

Cao *et al.* processed the abovementioned e,e,e-C<sub>60</sub> (COOEt)<sub>3</sub> (**42**), together with a diazonium resin, into a thin film

Scheme 15 Synthesis and incorporation of C<sub>60</sub>-tris-malonic acid derivatives in thin films.Fig. 3 e,e,e-Tris adduct **45** and its molecular structure.

(Scheme 15).<sup>61</sup> In the first step they formed a layer-by-layer ultrathin film by self-assembly of tris-carboxylate ion **42**<sup>3-</sup> and the diazonium moiety of the resin **43** into a poly(acrylic acid) (PAA) matrix through their electrostatic interaction. In a second step the film was annealed under UV irradiation by decomposition of the diazonium moieties and formation of covalent bonds leading to polymer **44**. The morphology of this film was studied by AFM/FFM experiments, which indicated its good load-bearing and friction properties. The film of polymer **44** showed good lubricative properties, due to its layered structure. Thus, it might be used as high performance lubricants in the future.

We recently showed that the CBr<sub>4</sub>-mediated non-tethered regioselective synthesis of higher fullerene-adducts developed by the Sun group is not limited to malonates.<sup>62</sup> In this regard, we reported e,e,e-tris adduct **45** bearing three dibenzoylmethane moieties (Fig. 3).<sup>63</sup> This compound was synthesized in 15% yield by reacting C<sub>60</sub> and dibenzoylmethane in presence



of DBU and 100 equiv.  $\text{CBr}_4$ . Furthermore, its molecular structure was proven by X-ray crystallography (Fig. 3). Tris-adduct **45** is a potential candidate for acceptor material in OPVs and a versatile building block for nano-structures due to its highly symmetric structure.

### 2.3. Tetrakis-functional fullerenes

Compared to the aforementioned mono, bis and tris-adducts, fullerene tetrakis-adducts play only a minor role. Nevertheless, they are useful building blocks due to their structural diversity and thus represent a highly interesting research field. As their regioselective synthesis cannot be controlled easily, rather complex synthetic routes are needed to gain access to tetrakis-substituted derivatives.

Facing these circumstances, the Diederich group developed a tether-based synthesis protocol that leads to malonate tetrakis-adducts **51** and **52** (Scheme 16).<sup>32</sup> First,  $\text{C}_{60}$  was reacted with tethering agent **46**, followed by addition of three diethyl malonate moieties (X in Scheme 16) to give mixed hexakis-adduct **47**. Then, under irradiation with a Hg lamp in the presence of  $\text{O}_2$ , dialcohol **48** was synthesized and further converted to compound **49**. Cleavage of the tethering ester groups gave symmetric tetrakis(diethyl malonate)-adduct **50** with all four substituents arranged along its equator belt. Its molecular structure was proven by X-ray crystallography (Fig. 4). Finally,

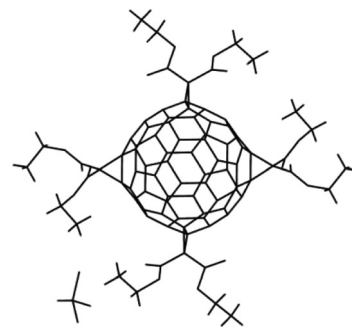
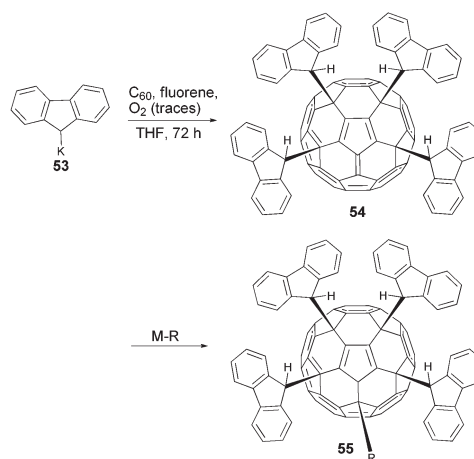


Fig. 4 Molecular structure of a tetrakis-substituted fullerene **50**.



Scheme 17 Synthesis of fulvene-like tetrakis-adduct **54**.

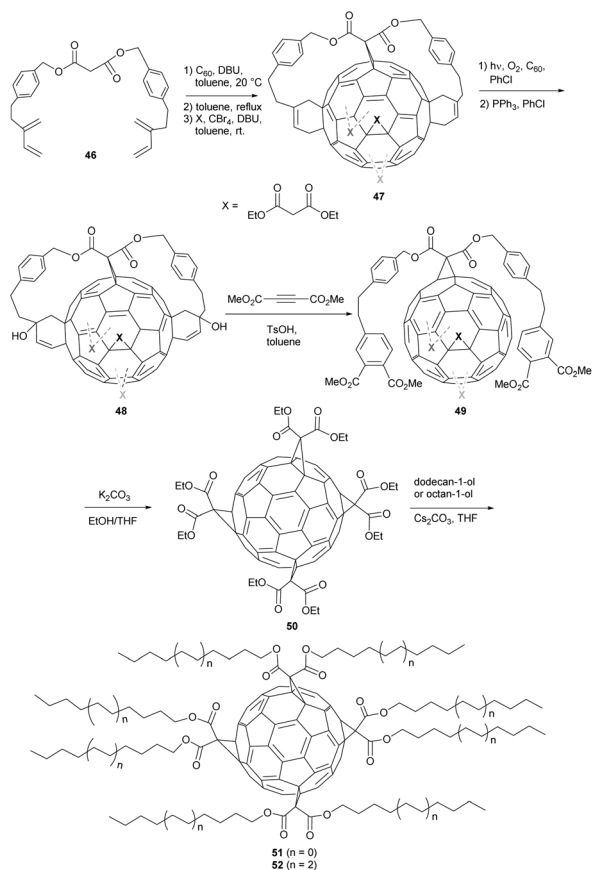
transesterification with either dodecan-1-ol or octan-1-ol gave long-chained derivatives **51** and **52** in 16% and 14% yield, respectively. As already mentioned above, such tetrakis-adducts bearing  $D_{2h}$  symmetry can act as potential building blocks, leading to highly functional and at the same time highly symmetric nano-structures with unprecedented properties.

One further interesting fullerene tetrakis-adduct having a fulvene-like  $\pi$ -system was reported by Murata *et al.* (Scheme 17).<sup>64</sup> Through the reaction of  $\text{C}_{60}$  with potassium fluorene (**53**) in the presence of fluorene and traces of  $\text{O}_2$ , compound **54** was obtained in 40% yield as black crystals whose structure was elucidated by X-ray crystallography (Fig. 5).

The authors demonstrated the fulvene reactivity of this system by reacting it with nucleophiles such as potassium fluorene **53**, lithium organyls or NaCN to obtain the corresponding pentakis-adducts **55** bearing five substituents arranged in a propeller-like fashion.

### 2.4. Pentakis-functionalized fullerenes

Penta-functional adducts of Buckminsterfullerene have been reported mainly with a focus on pentahaptofullerene and its metal complexes. The fullerene analogues of cyclopentadiene



Scheme 16 Synthetic route to tetrakis-functional fullerenes.



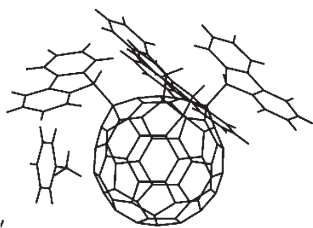
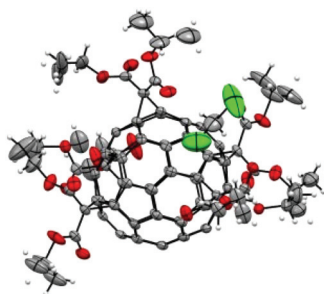
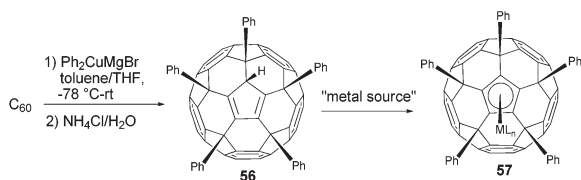
Fig. 5 Molecular structure of a tetrakis(9-fluorenyl)fullerene **54**.<sup>64</sup>

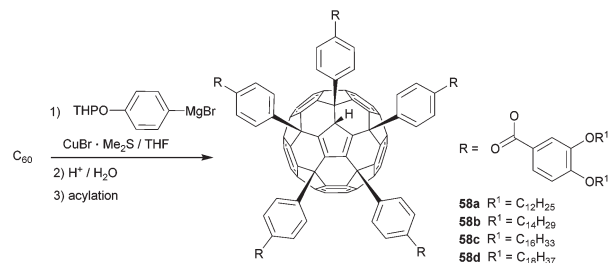
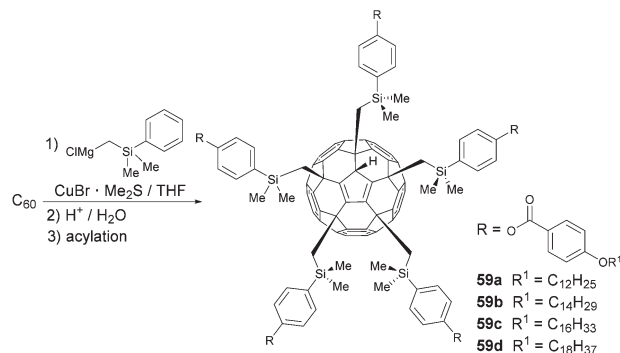
Fig. 6 Molecular structure of a pentakis-substituted fullerene.

Scheme 18 Synthesis of pentahaptofullerene  $C_{60}Ph_5H$  (**56**).

and its anion are obtained by five-fold addition reaction between organocopper compounds and  $C_{60}$  (Fig. 6).

The field of such pentahapto fullerenes and their metal complexes has been intensely studied by Sawamura and Nakamura's group. They found that unlike organolithium or Grignard reagents, cuprates can undergo a five-fold addition onto  $C_{60}$  yielding Cp-like ligands.<sup>34</sup> In that context  $C_{60}$  was reacted with an excess amount of  $Ph_2CuMgBr$  and  $C_{60}Ph_5H$  (**56**) was obtained in 94% yield after quenching with aqueous  $NH_4Cl$ . Furthermore,  $\eta^5$ -metal complexes **57** were formed, proving the applicability of fullerene **56** as a cyclopentadiene analogue (Scheme 18). Although this compound bears a Cp-ring that is separated from the remaining  $C_{50}$ - $\pi$ -system by five  $sp^3$  carbon atoms, UV-vis spectroscopy of both compound **56** and the corresponding thallium complex indicates that the electronic properties of parental  $C_{60}$  were not severely affected by the pentakis-functionalization. Thus, such fullerene derivatives combine the ability to stabilize numerous metals in a wide range of oxidation states with the outstanding optoelectronic properties of  $C_{60}$ . This may lead to new materials with a remarkable application potential in different fields.

Sawamura *et al.* combined the aforementioned concept of fullerene-based Cp-derivatives with supramolecular

Scheme 19 Synthesis of liquid-crystalline  $C_{60}$ -pentakis-adducts.

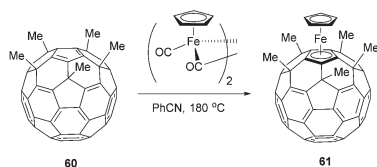
Scheme 20 Pentakis-adducts bearing a cup-shaped cavity.

chemistry.<sup>17</sup> In a three-step protocol consisting of the initial pentakis-functionalization of  $C_{60}$  with  $(4-(THPO)C_6H_4)_5CuMgBr$  followed by deprotection of the alcohol moiety and subsequent acylation, they synthesized pentakis-adducts **58a–d**, in about 60% overall yield (Scheme 19).

The five biaryl rests arranged around one five-membered ring of the  $C_{60}$  cage create a deeply conical cavity, perfectly suited for the incorporation of a second fullerene molecule through  $\pi$ - $\pi$  interactions. The latter leads to one-dimensional stacking of these shuttlecock-shaped molecules to give supramolecular columns, which was proven by small-angle (SAXD) and wide-angle X-ray diffraction (WAXD). Due to the flexible aliphatic side chains, these assemblies show thermotropic and lyotropic liquid crystalline behaviour.

In a related report from the same group, the biaryl moieties were not connected directly to  $C_{60}$  like in compounds **58a–d**, but *via* additional  $CH_2SiMe_2Ar$ -linkers (Scheme 20, compounds **59a–d**).<sup>65</sup> The authors used a similar synthetic strategy as described above, except with the addition of cuprate  $(4-(THPO)C_6H_4SiMe_2CH_2)_5CuMgCl$  as the key step. Their investigation by DSC, polarizing optical microscopy and X-ray diffraction revealed that the cavities now are larger and more cup-shaped due to the rather long Si–C bond. Thus, in the supramolecular assemblies of compounds **59a–d**, the fullerene site of a given molecule perfectly fits into the cavity of its neighbour, which allows for higher fullerene–fullerene interaction. Furthermore intracolumnar distances are shorter than in compounds **58a–d**.





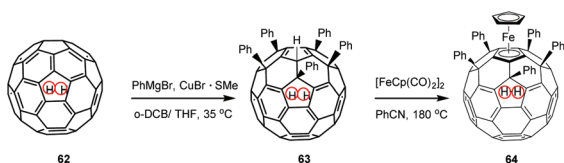
**Scheme 21** Synthetic route to a fullerene/ferrocene hybrid.

Since in  $R_5C_{60}H$  structures the optoelectronic properties of parental  $C_{60}$  remain unaffected, compounds **58a–d** and **59a–d** represent a unique material class that unites the features of fullerenes, Cp-ligands and liquid crystals. For example, by complexing the Cp-moieties with metals, unprecedented redox-active liquid-crystalline fullerene/metal hybrid materials could be created in the future.

This issue was impressively addressed again by Sawamura *et al.*, who reported fullerene/ferrocene hybrid material  $Fe(C_{60}Me_5)Cp$  (**61**) (Scheme 21).<sup>66</sup> This 18-electron sandwich complex is accessible through direct complexation of  $C_{60}Me_5H$  (**60**) with  $[FeCp(CO)_2]_2$  in 52% yield.

The molecular structure of complex **61** was elucidated by X-ray diffraction, revealing a staggered conformation of the free (Cp) and the fullerene-bound (FCp) cyclopentadienyl units. As the Cp–Fe–FCp distances are very similar to those of ferrocene, both the Cp and the FCp units must be aromatic. This is additionally confirmed by NMR spectroscopy. Furthermore in the  $^1H$  NMR all proton resonances are notably shifted downfield compared to ferrocene, which indicates the highly electron withdrawing character of  $C_{60}$ . The EPR spectrum of compound **61** did not show any peak, which indicates a singlet ground state like in ferrocene, whereas the UV/vis spectrum looks similar to that of pristine  $C_{60}$ . Finally, CV measurements revealed both a ferrocene-like reversible oxidation potential (+0.22 V) and a fullerene-like reversible reduction potential (1.46 V *versus* ferrocene). With these findings the authors clearly showed that complex **61** is a fullerene/ferrocene hybrid material, comprised of both the electronic properties of pristine ferrocene and fullerene. Since various protocols exist to either modify the ferrocene or the fullerene unit, these structures can make tailored materials accessible and therefore serve as key compounds in material science.

Matsuo *et al.* investigated the corresponding pentakis-adducts of the endohedral fullerene  $H_2@C_{60}$  (**62**).<sup>67</sup> Following the above mentioned cuprate addition protocol, they synthesized endohedral pentakis-adduct **63** in 92% yield by reacting  $H_2@C_{60}/C_{60}$  (4/1) with 15 equiv. of the cuprate prepared *in situ* from  $PhMgBr$  and  $CuBr \cdot SMe_2$  (Scheme 22). Compound



**Scheme 22** Endohedral pentakis-adduct and fullero-ferrocene.<sup>67</sup>

**63** was then converted by treatment with  $[FeCp(CO)_2]_2$  to the corresponding ferrocene derivative **64** in 71% yield. X-Ray diffraction experiments revealed that the encapsulated dihydrogen has no influence neither on the molecular nor the crystal structure, when compared to those of the corresponding non-hydrogen-containing derivative. Furthermore the authors demonstrated that in compounds **63** and **64** the  $^1H$  NMR resonance of the encapsulated  $H_2$  was remarkably upfield-shifted (10.39 ppm and 9.79 ppm, respectively), compared to endohedral fullerene **62** (1.44 ppm). The authors assigned these effects to shielding/deshielding effects inside the fullerene core, due to a disturbance of the parental  $C_{60}\pi$ -system caused by outer sphere functionalization. In summary, since  $H_2$  encapsulated in  $C_{60}$  has only neglectable influence on its physical and chemical properties and its  $^1H$  NMR resonance responds sensitively to changes on the outer sphere, it can act as a sensing probe to the inside and outside environment of the cage and therefore provide deep insight into electronic properties of functionalized fullerenes.

## 2.5. Hexakis-functionalized fullerenes

The bonds between two fused six-membered rings in  $C_{60}$  display the most pronounced double bond character as they are shorter than the other bonds and thus the most reactive. Such bonds theoretically allow to access to highly substituted products of  $C_{60}$ . Many hexa-substituted products were accessible through a wide range of reactions and with different symmetry patterns. For instance, the reaction of fullerene  $C_{60}$  with *tert*-butyl hydroperoxide in the presence of ceric ammonium nitrate (CAN) yields hexakis-adduct **65** (Fig. 7), which is a starting material to isomerically pure fullerenols.<sup>68</sup> Star-like water soluble fullerene derivatives can be synthesized by the reaction of  $C_{60}$  with sodium naphthalide, followed by nucleophilic substitution on 1,4-butane sultone to give hexa(sulfobutyl)-fullerene  $C_{60}[(CH_2)_4SO_3]_6^-$ . This compound found many applications such as MALDI matrix,<sup>69</sup> free radical scavenger,<sup>70</sup> or water-soluble electron-accepting layer for photocurrent generation.<sup>71,72</sup>

Hexakis-substituted fullerenes with an octahedral addition pattern are highly symmetrical three-dimensional structures that have therefore attracted much attention for a diverse range of applications. Two early X-ray structures for hexa-substituted fullerenes are depicted in Fig. 8.

The first examples of octahedral fullerene synthesis appeared in the literature at the beginning of the 90's. A  $C_{60}$  core bearing six octahedrally-arranged  $[(C_2H_5)_3P]_2Pt$  groups (each bound in a dihapto manner) and having overall  $T_h$  point group symmetry was synthesized in 88% yield in a one step

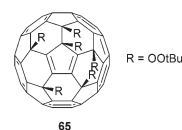


**Fig. 7** Hexa-substitution of  $C_{60}$  with *tert*-butylperoxy radicals.





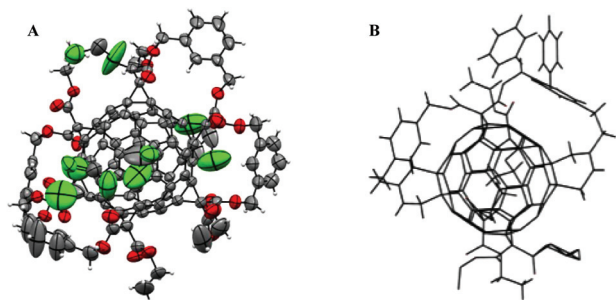
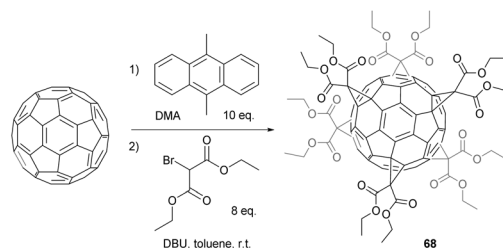


Fig. 8 Molecular structure of A (66): a hexakis-substituted fullerene (CCDC 145416)<sup>35</sup> and B (67): a tethered hexakis-substituted fullerene (CCDC).<sup>38</sup>

process involving  $C_{60}$  and 10 equivalents of  $[(C_2H_5)_3P]_4Pt$  in benzene.<sup>73</sup> The structure of this air sensitive product was unambiguously determined by NMR spectroscopy as well as X-ray crystallography. The high degree of regioselectivity is assumed to occur due to reversible metal complexation, slowly equilibrating in favour of the thermodynamic product. Later, Kräutler *et al.* reported that the Diels–Alder reaction is also a suitable route to access highly symmetrical octahedral fullerene products, since 2,3-dimethyl-1,3-butadiene was efficiently connected to the fullerene core through six regioselective  $[4 + 2]$ -cycloaddition reactions producing the expected compounds in 28% yield.<sup>74</sup> The preparation of hexa-substituted  $C_{60}$  derivatives bearing six pyrrolidine peripheral groups has been achieved by 1,3-dipolar cycloaddition between  $C_{60}$  and azomethine ylides.<sup>75</sup> This reaction led to the formation of two hexa-substituted products, one with the  $T_h$  symmetry and one with a  $D_3$  symmetry, both displaying high fluorescence quantum yields that suggest their applicability in electroluminescent devices and light-harvesting dendritic systems.

The Bingel cyclopropanation approach for  $C_{60}$  functionalization has also been considered as a potential way to access hexa-substituted derivatives, since it deals with irreversible reactions that deliver stable derivatives. Hirsch *et al.*<sup>76</sup> reported a remarkable stepwise synthesis starting from the chiral  $C_3$ -symmetric tris-adduct whose synthesis was previously reported.<sup>51</sup> Successive equatorial (*e*) additions of diethylbromomalonates in the presence of sodium hydride afforded first the  $C_s$ -symmetric tetrakis-adduct, followed by the  $C_{2v}$ -symmetric pentakis-adduct and finally the  $T_h$ -symmetric hexakis-adduct. It is worth noting that each of the intermediates as well as the final hexa-substituted product were isolated by tedious and scale-limiting HPLC purification. Furthermore, the overall synthetic route afforded the expected hexakis-substituted product with a total yield of 0.2% from  $C_{60}$ . In the meantime, Diederich *et al.* reported the syntheses of other hexakis-adducts that were obtained through an original tether-directed remote functionalization concept.<sup>77</sup> Next, Lamparth *et al.* developed a one-step route with good yields to hexa-substituted  $C_{60}$  derivatives from  $C_{60}$  and malonates. This route is based on template-directed activation of the octahedral reactive positions of the fullerene core.<sup>36</sup> In the first step,  $C_{60}$  was



Scheme 23 First one-step synthesis of hexa-substituted  $T_h$  fullerene 68 from diethylbromomalonate.

reacted in a reversible way with 9,10-dimethylantracene (DMA, 10 equiv.) to form the corresponding Diels–Alder adducts of the general formula  $C_{60}(DMA)_n$  (Scheme 23).

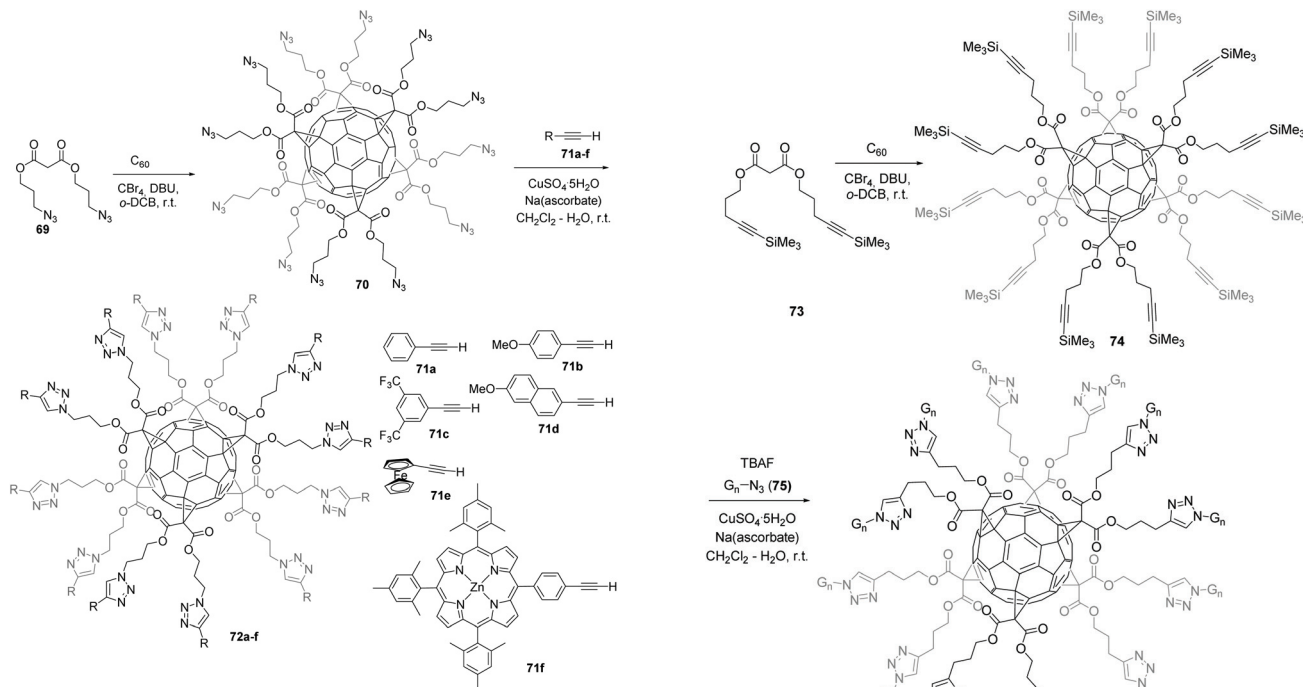
Thus, subsequent treatment with DBU as a base and diethylbromomalonate allowed the formation of the expected hexakis-substituted product 68 in 37% isolated yield, which is 120 times better than the step-by-step approach previously developed. Interestingly, the authors showed that 68 could be quantitatively transformed into the corresponding highly water-soluble hexamalononic acid derivative by treatment with NaH in methanol. Later on, Hirsch *et al.* further improved the reaction conditions when they found that bromomalonates, which are difficult to prepare and isolate as pure materials due to their complicated structures, could be simply generated *in situ* by using 10 equiv. of both the starting malonates and  $CBr_4$  as the bromination agent.<sup>78</sup>

Importantly, the research group of Sun has recently brought further improvements to the above-mentioned reaction conditions, which are now the more appropriate method to generate a wide range of octahedral fullerene derivatives from  $C_{60}$  in one step and high yield.<sup>62,79</sup> This was achieved by a simple modification of the reaction conditions involving the use of a large excess of bromination agent (100 equiv. of  $CBr_4$ ) without the need of DMA as templating agent and resulted in a dramatic increase of the final hexakis-substituted product yield.

While very useful and despite its many optimizations, the synthetic approach consisting of a one-pot regioselective installation of six malonates entities onto the fullerene core results in low yield and limited purification when starting with bulky and structurally more complicated malonates. To overcome this general trend, different research groups developed a range of synthetic strategies over the last few years to deal with the synthesis of “simple”  $C_{60}$  hexakis-adduct in one step, bearing peripheral reactive groups, that could be further functionalized. To do so, the later reaction must be easy to perform, tolerant to a wide range of functional groups, high yielding and should not produce many by-products for ease of purification.

The Nierengarten group was the first to report on such an approach and evaluated the potential of the copper-mediated Huisgen 1,3-dipolar cycloaddition click reaction to perform further functionalization of fullerene hexakis-adducts. Iehl *et al.* reported the synthesis of malonate 69 (Scheme 24)

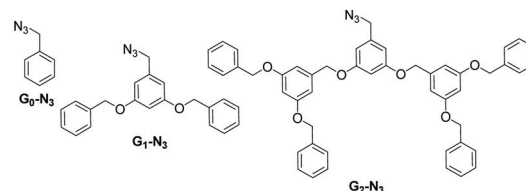




**Scheme 24** Synthetic route to highly functionalized [60]fullerene hexakis-adducts by Click chemistry.

bearing two terminal azide functional groups.<sup>80</sup> Briefly, the latter was easily obtained in two steps by the reaction of malonyl dichloride with 3-bromopropan-1-ol in the presence of pyridine and subsequent treatment with sodium azide in DMF at room temperature.<sup>80</sup> Hexakis-adduct **70** was then readily synthesized by the reaction of  $C_{60}$  with **69**,  $CBr_4$  and DBU in *o*-DCB at room temperature for 72 h. The product was obtained as a pure material in 62% yield after silica-gel chromatography. The reaction conditions for the 1,3-dipolar cycloaddition of hexa-substituted fullerene **70** with various aryl alkynes **71a-f** were optimized, and products **72a-f** were obtained in 56–81% isolated yield by using the best conditions ( $CuSO_4 \cdot 5H_2O$  and sodium ascorbate in a mixture of  $CH_2Cl_2$ – $H_2O$  at room temperature). The authors proved the high efficiency of this two-step synthetic approach to easily obtain a wide range of highly functionalized octahedral fullerene hexakis-adducts, even with bulky peripheral groups.

Next, Iehl *et al.* reported the complementary version of the above mentioned twelve click reactions around the  $C_{60}$  core by preparing a  $C_{60}$  hexakis-adduct with twelve trimethylsilyl (TMS)-protected alkyne groups, which is suitable for further click reactions in the presence of various azide derivatives (Scheme 25).<sup>81</sup> Malonate **73** was accessible starting from malonyldichloride and the corresponding alcohol in the presence of pyridine. Hexakis-adduct **74** was then readily synthesized in 49% yield by the reaction of  $C_{60}$  with **73**,  $CBr_4$  and DBU in *o*-DCB at room temperature. The authors also showed that the Huisgen coupling could be directly conducted from protected-alkyne **73** by *in situ* desilylation in the presence of TBAF,  $G_n-N_3$  (**75**,  $n = 0-2$ ),  $CuSO_4 \cdot 5H_2O$ , and sodium ascorbate in  $CH_2Cl_2$ –



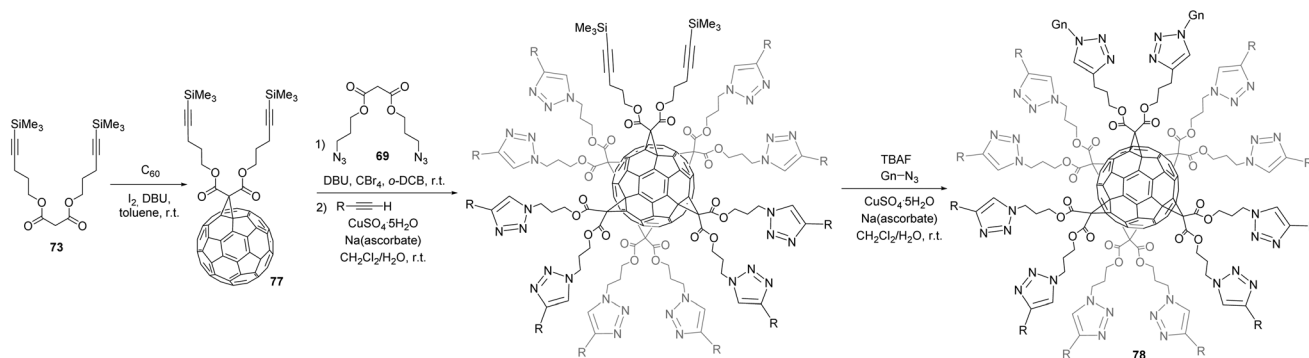
**Scheme 25** Alternative synthetic approach to access highly functionalized hexakis-adducts by click derivatization.

$H_2O$  at room temperature. Under these conditions, products **76a-c** were isolated in excellent yields ranging from 58 to 84%.

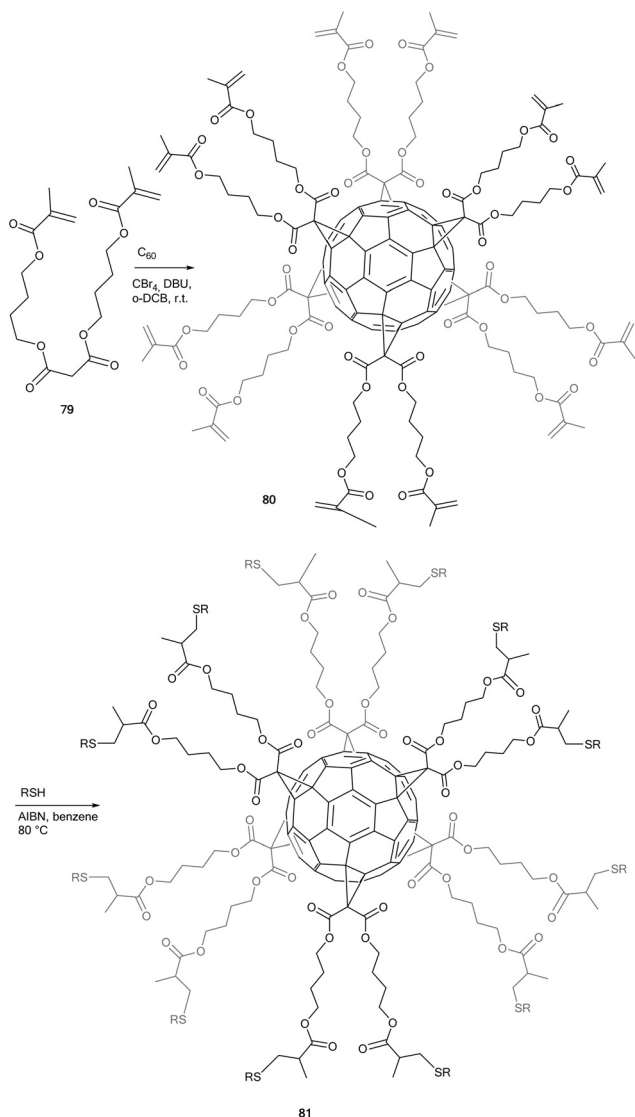
Furthermore, the authors demonstrated that by using a step-wise combination of these complementary click approaches, [5:1]fullerene hexakis-adducts with various peripheral groups are accessible (Scheme 26). To this end,  $C_{60}$  hexakis-adduct bearing two TMS-protected alkynes and ten azide groups has been described. Fullerene mono-adduct **77** was first prepared in 53% yield and further reacted with an excess of complementary malonates to yield the corresponding [5:1]fullerene hexakis-adducts in 45% yield. Hence, successive Huisgen reactions were conducted to afford the expected derivative **78** in good to excellent yields.

Iehl *et al.* further enriched the functionalization possibilities on fullerene hexakis-adducts by using the well-documented radical thiol–ene chemistry (Scheme 27).<sup>82</sup> Thus, malonate **79** was efficiently linked to the fullerene core by the modified-Bingel cyclopropanation method allowing access to hexakis-adduct **80** in 41% isolated yield. Next, the desired thioether derivatives **81** were obtained by using a mixture of **80**, RSH (20 equiv.) and AIBN (3 equiv.) in degassed-benzene at 80 °C





**Scheme 26** Synthetic route to [5:1]hexakis-adducts of  $C_{60}$  by a sequential click-click approach.



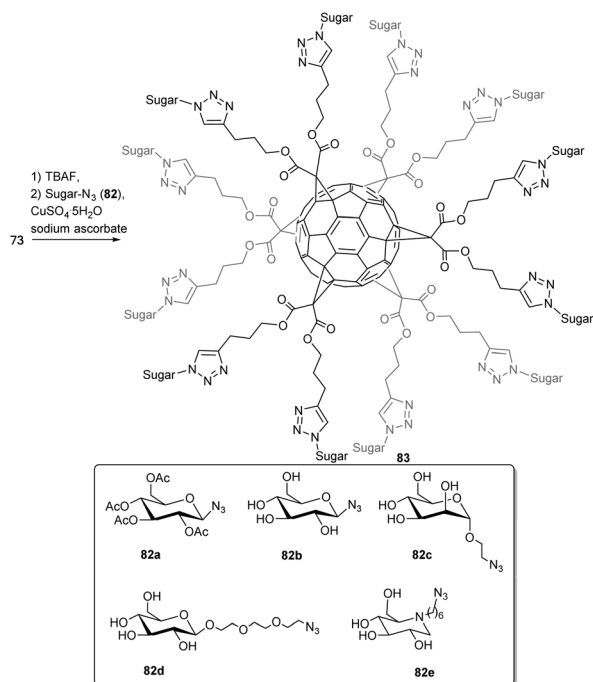
**Scheme 27** Thiol-ene reactions for hexakis-substituted fullerene derivatization.

for 1 h. Using this approach, fullerene hexakis-adducts were obtained in 30–50% yields.

Based on the efficiency of the derivatization methods previously described on fullerene hexakis-adducts, the authors were even able to produce building blocks incorporating complementary reactive centres with three different peripheral reactive sites (azide, TMS-protected alkyne and alkenes) and to selectively react each of them stepwise. Since the Click reactions (thiol-ene and Huisgen cycloaddition) used for the functionalization of the fullerene core are tolerant to a wide range of functional groups, this methodology allowed for the easy preparation of a large variety of unprecedented globular multifunctional nanomaterials with a controlled distribution of functional groups on the spherical framework, that could be useful for various applications.

For instance, Nierengarten *et al.* developed an efficient access to fullerene hexakis-adducts derivatives bearing twelve peripheral carbohydrate moieties, to access a potential multivalent effect from cooperative interactions of the carbohydrate groups with the corresponding receptors, such as proteins.<sup>82</sup> Synthetic access to such compounds was accomplished by the copper-mediated Huisgen 1,3-dipolar cycloaddition between the sugar, bearing an azide functional group, and the corresponding hexakis-adduct bearing twelve terminal alkyne units, as shown in Scheme 28. Interestingly, the authors showed that instead of a two-step synthetic process, the conjugates could be even accessible in a one-pot reaction involving *in situ* desilylation with TBAF, followed by subsequent click reaction with the corresponding azide (13 equiv.) in the presence of  $CuSO_4 \cdot 5H_2O$  (0.1 equiv.) and sodium ascorbate (0.3 equiv.) in DMSO at room temperature. Following this novel synthetic route, the authors synthesized a series of new fullerene glycoconjugates with high isolated yields ranging from 40% to 90% yield. They further demonstrated that the synthetic access to fullerene sugar balls could be achieved in a reverse approach between a fullerene building block bearing twelve terminal azides as functional groups and various sugar moieties bearing terminal alkynes. Thus, it was shown that fullerene hexakis-adducts bearing twelve peripheral carbohydrate moieties can be synthesized in good yields by grafting unprotected





Scheme 28 Synthetic route to fullerene (imino)sugar balls.

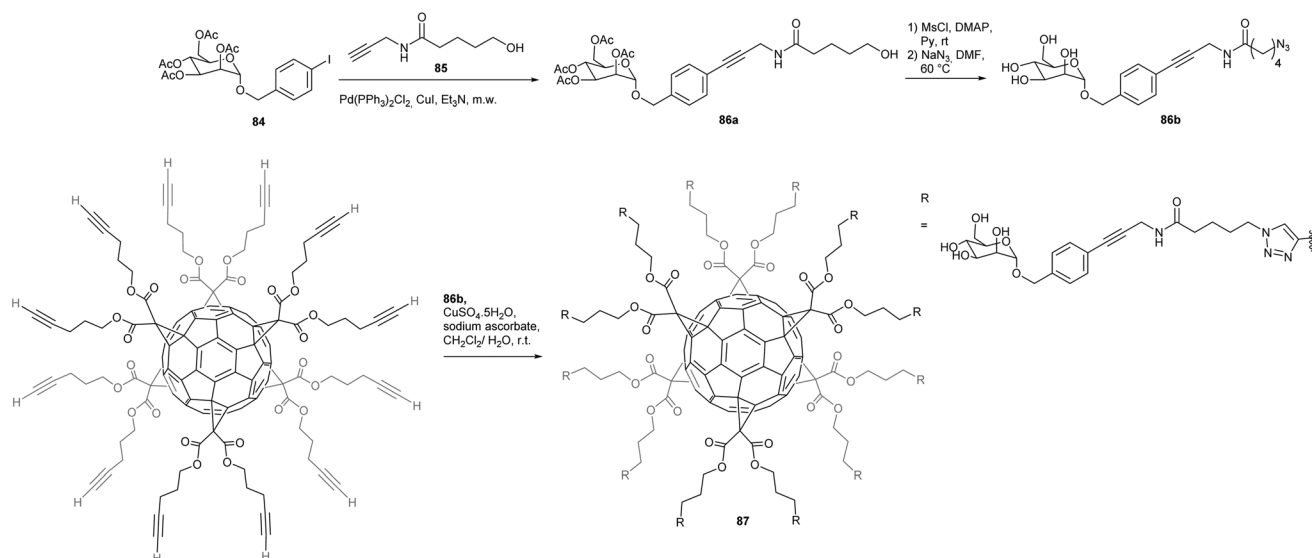
sugar derivatives onto the fullerene core by efficient Huisgen-type click reactions.

By this synthetic route, Compain *et al.* reported the synthesis of a fullerene hexakis-adduct, decorated with twelve iminosugar residues **82** in up to 83% yield, with the intent of studying the potential of multivalency on enzyme inhibition.<sup>9</sup> The inhibition profile of this fullerene iminosugar ball has thus been systematically evaluated against various glycosidases and compared with its monovalent analogue. The results indicated a dramatic and unprecedented multivalent effect.

Indeed, for most of the glycosidases tested, hexakis-substituted fullerene obtained from iminosugar **82e** demonstrated a better binding activity than the corresponding monomer. The stronger multivalent effect was obtained with Jack bean  $\alpha$ -mannosidase, which had a  $K_i$  value up to three orders of magnitude higher than the monomeric control iminosugar. These results highlighted the impact of the central  $C_{60}$  scaffold on the inhibition potential of the multivalent architecture.

It has also been reported that fullerene glycoconjugates have interesting applications in antibacterial therapy.<sup>10</sup> Bacteria adhere in the early stages of infection to the cell membrane by interactions between carbohydrate present at the surface of epithelial cells and some proteins such as adhesin present on the tip of bacterial pili.

The group of Nierengarten studied dodecamannosylated fullerenes and their interactions with *Escherichia Coli* adhesion FimH, which is a particular lectin for which no multivalent effects have been reported so far, in contrast to other lectins that are mostly multimeric.<sup>9,82</sup> The key intermediate bearing an azide functionality was thus prepared by a Sonogashira cross-coupling reaction between mannoside **84** and alkyne **85** in 77% yield (Scheme 29). The latter product was then converted into the desired azide precursor **86a**, in three steps involving first a mesylation step, followed by the substitution with sodium azide and finally, the removal of the acetyl groups using the Zemplén deprotection method. The last step consisted in the efficient coupling of azide **86b** with a fullerene bearing twelve terminal alkyne functionalities to produce the desired mannosylated hexakis-substituted fullerene product **87** having a benzylic aromatic ring at the anomeric position and an amide linker. The ligand potential of this compound towards bacterial adhesin FimH was assessed by isothermal titration calorimetry (ITC), surface plasmon resonance (SPR) and hemagglutination assays. An unexpected phenomenon occurred during the usual titration of FimH by the dodeca-



Scheme 29 Synthetic access to dodecamannosylated fullerenes.





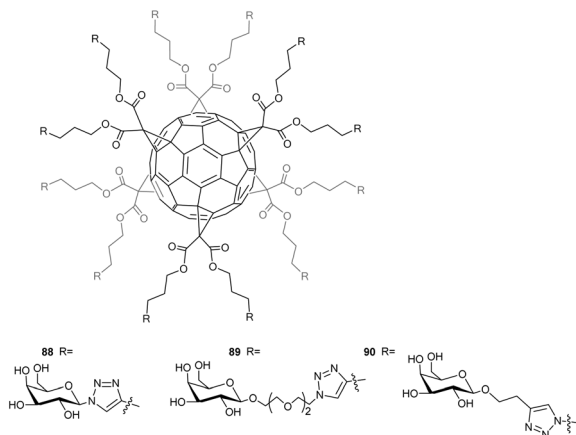


Fig. 9 Structures of hexakis-substituted fullerene-based glycoclusters.

mannosylated fullerene. Instead of the typical sigmoidal plot, the authors observed a first binding event followed by a strong exothermic jump that could be attributed to an aggregation of the protein. SPR thus confirmed the ITC findings that dodecamannosylated fullerene **87** can accommodate up to seven lectins. It was further demonstrated that the length and the structure of the anomeric substituent are key factors that dramatically enhance the binding affinity of the carbohydrate subunit. This fullerene derivative also displayed a low micromolar inhibition level: in each case lower than its corresponding monomer. Thus, the authors proved that a globular  $C_{60}$  bearing peripheral mannose moieties can accommodate up to seven FimH molecules and thus have a strong affinity to FimH through multivalent effects. The multivalency has been recently corroborated by the Nierengarten group.<sup>83,84</sup>

As an extension of the above-cited results, Cecioni *et al.*<sup>12</sup> reported a preparation of dodecavalent glycoclusters bearing galactose and peripheral glucose residues (Fig. 9) and studied their interactions with lectin PA-IL (LecA), a bacterial lectin from *Pseudomonas Aeruginosa*. This bacterium is a target of choice as it is responsible for nosocomial infections and is displaying increasing resistance to antibiotics. Interactions between PA-IL and carbohydrates, particularly galactose, are at the origin of this bacterial infection. It was thus anticipated that strong ligands of lectin could be valuable drugs against bacterial infections.

Following the same synthetic pathways described previously, the synthesis of compounds **88**, **89** was achieved from the hexakis-substituted fullerene derivative bearing twelve silylated alkyne moieties. This derivative was first treated with TBAF, yielding terminal alkyne moieties, available to undergo Click reaction with the galactoside counterparts containing terminal  $N_3$  groups catalysed by  $CuSO_4 \cdot 5H_2O$  and sodium ascorbate to obtain compound **88** in 74% and **89** in 72% yield. A reverse approach was used to synthesize compound **90** in 73% yield by conjugating the dodecaazide derivative with the corresponding carbohydrate precursor bearing a terminal alkyne functional group. These compounds were then analysed as inhibitors of the bacterial lectin PA-IL by using hemaggluti-

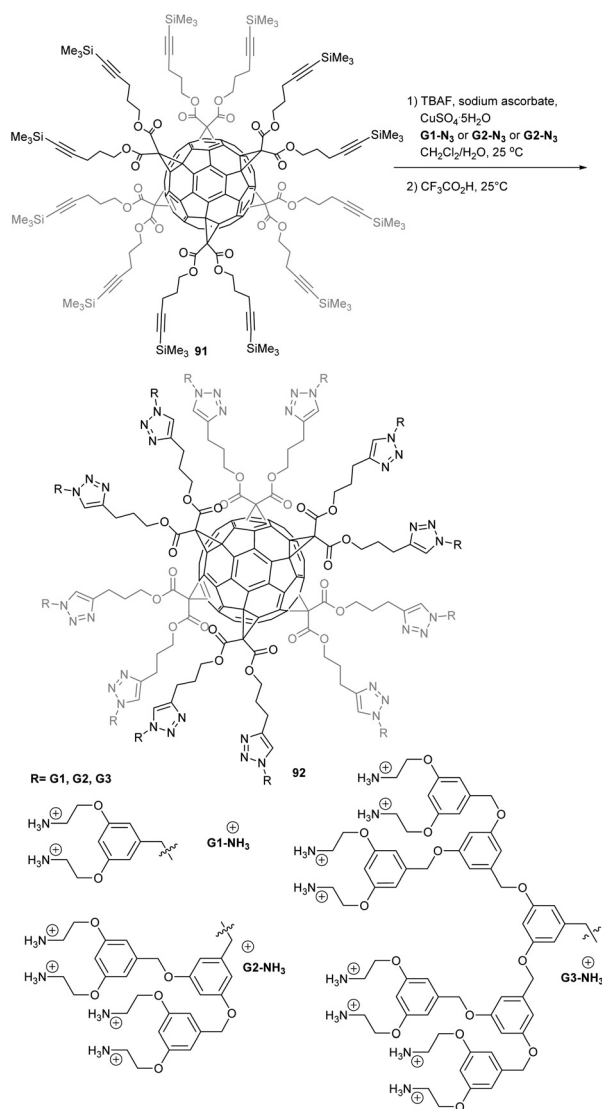
nation inhibition assays, enzyme-linked lectin assays and surface plasmon resonance assays. The level of inhibition or binding was found to be highly dependent on the nature of the peripheral sugar residues (galactose *vs.* glucose) and the nature of the spacer separating the galactose residues from the fullerene core. Importantly, the peculiar spherical distribution of the twelve sugar subunits around the carbon sphere led to a dramatic multivalent effect. Galactosylated fullerene derivatives **90** display up to a 12 000-fold increase in binding affinity compared to the monovalent carbohydrate reference. These fullerene derivatives have the highest reported binding affinity in terms of ligand of lectin to date and thus represent potential new anti-adhesive agents against bacterial infection. A recent review written by Nierengarten *et al.* gives further reference to the biological potential of fullerene sugar balls.<sup>85</sup>

The multivalent potency of hexakis-substituted fullerene derivatives have also been evaluated as a potential precursor to non-viral gene delivery vehicles. To do so, Sigwalt *et al.*<sup>11</sup> synthesized different polycationic fullerene hexakis-adduct derivatives bearing cationic  $NH_3^+$  terminal groups with the general structure **Gn-3NH<sub>3</sub><sup>+</sup>**, as depicted in Scheme 30.<sup>11</sup> Precursors **Gn-3N<sub>3</sub>** were obtained from the corresponding benzylic bromides treated with  $NaN_3$  in DMF. The subsequent grafting of azides **Gn-3N<sub>3</sub>** ( $n = 1, 2$  or  $3$ ) onto the hexa-substituted fullerene core was achieved under copper-catalyzed alkyne-azide 1,3-dipolar cycloaddition conditions. Treatment of fullerene hexakis-substituted building block **91** with a slight excess of azides  $GnN_3$  in the presence of TBAF,  $CuSO_4 \cdot 5H_2O$  and sodium ascorbate gave the corresponding benzyloxycarbonyl (Boc)-protected dendrimers **GnNH(Boc)** ( $n = 1, 2$  or  $3$ ) in remarkable isolated yields. Finally, treatment of **G1-3NH(Boc)** with a large excess of trifluoroacetic acid (TFA) gave the corresponding deprotected derivatives **G1-3NH<sub>3</sub><sup>+</sup>** as their trifluoroacetate salts in quantitative yields.

As a first set of evaluation, the authors showed that polycationic fullerene **G1-3NH<sub>3</sub><sup>+</sup>** complexes efficiently plasmidic DNA at N/P ratio of 2, forming “donut-like” polyplex structures with diameters smaller than 100 nm. Next, pCMV-Luc gene delivery experiments were conducted with **G1-3NH<sub>3</sub><sup>+</sup>** polyplexes on cultured HeLa cells. While **G1-NH<sub>3</sub><sup>+</sup>** is only slightly active in delivering DNA to the cells, **G2-NH<sub>3</sub><sup>+</sup>** and **G3-NH<sub>3</sub><sup>+</sup>** display approximately the same gene delivery capacity as commercially available JetSI-ENDO, with comparable luciferase expression level, at N/P ratio of 2 (*i.e.* between  $10^{11}$  and  $10^{12}$  RLU per mg of protein). Moreover, the most active derivative **G2NH<sub>3</sub><sup>+</sup>** had minimal toxicity effects as revealed by the amount of total proteins that only diminished from 10% of its initial amount in untreated cells at the optimal N/P ratio for transfection. These results showed for the first time that polycationic fullerene hexakis-adducts could be efficient synthetic gene transfection vectors for DNA delivery with low toxicity despite a high density of cationic charges around the  $C_{60}$  core. No siRNA delivery has been reported with this system to date, or *in vivo* delivery experiments.

Based on the unique  $T_h$  octahedral symmetry of hexa-substituted fullerene derivatives, researchers have been interested





**Scheme 30** Synthetic route to polycationic fullerene hexakis-adducts.<sup>12</sup>

in studying whether hexakis-substituted fullerene could be a suitable scaffold to graft redox entities on the periphery to identify charge hopping from one redox centre to another by ultrafast cyclic voltammetry. With this idea in mind, Fortgang *et al.* synthesized the desired [5:1]fullerene hexakis-adduct by a stepwise functionalization of the hexa-substituted fullerene scaffold with sequential copper(i)-catalyzed alkyne–azide cycloaddition reactions, which allowed the successive grafting of two kinds of peripheral groups: ferrocene redox subunits and 1,2-dithiolane moieties available for grafting onto the gold electrode (Scheme 31).<sup>86</sup>

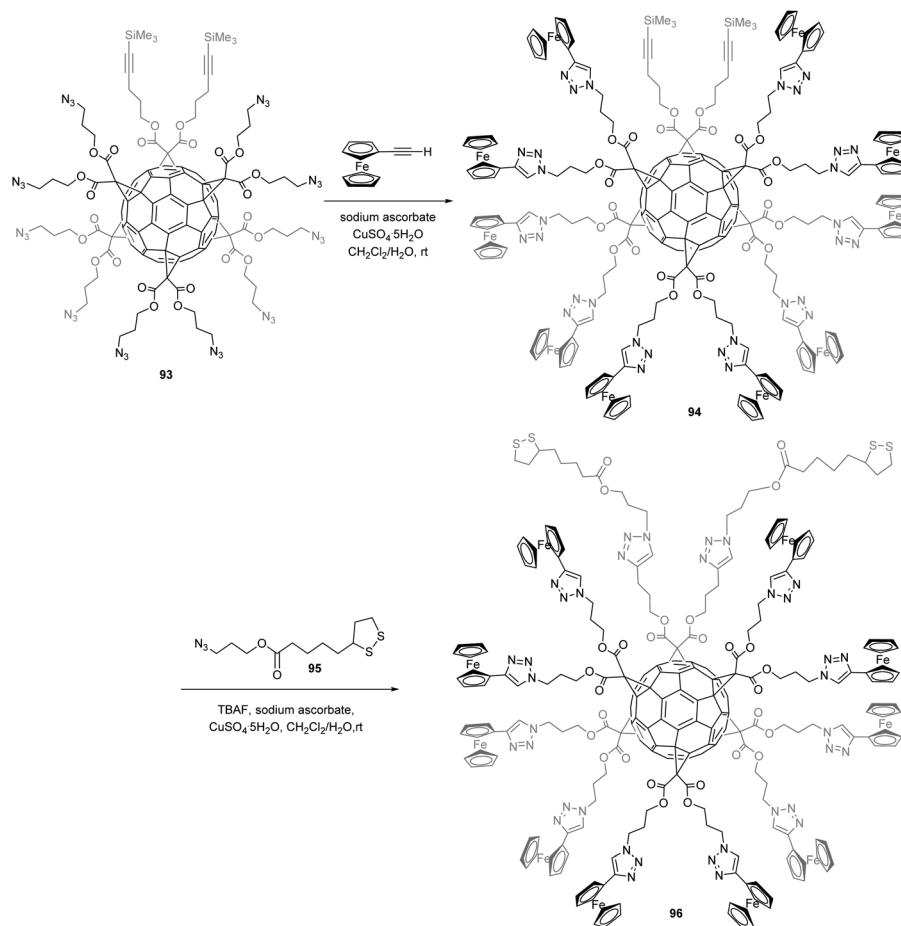
Reaction of starting block **93** with ethynylferrocene in the presence of  $\text{CuSO}_4 \cdot 5\text{H}_2\text{O}$  and sodium ascorbate gave compound **94**. Subsequent treatment with azide **95** in the presence of TBAF,  $\text{CuSO}_4 \cdot 5\text{H}_2\text{O}$ , and sodium ascorbate in a  $\text{CH}_2\text{Cl}_2$ – $\text{H}_2\text{O}$  mixture afforded the fully reacted [5:1]fullerene hexakis-adduct **96**. By usual techniques, this mixed [5:1]fullerene hexakis-

adduct was immobilized onto gold ultramicroelectrode due to its dithiolane groups, which allow the ten peripheral ferrocene redox subunits to spatially organize on the surface of the electrode with a certain degree of control by the rigidity of the  $\text{C}_{60}$  core. The first oxidation wave of the compound **96**, related to oxidation of the ferrocene entities, has been mainly studied. Indeed, at low scan rates, ferrocene entities that lie too far away from the surface cannot communicate directly with the electrode since the electronic coupling is too weak. These ferrocene moieties can however be oxidized in a multistep hopping mechanism, which results from redox centres that interact with one another. At high scan rate, the waves broaden and the peak potentials shift a little because the voltammetric rate compares to the one related to electron transfer between the electrode and the redox sites in its proximity. The results gave an indication that only a fraction of the ferrocene subunits of **96** are oxidized during the forward scan. This results from that some redox centres nearby the electrode remain independent, with pure adsorption behaviour, no electron hopping.<sup>86</sup>

By the same synthetic approach described above involving sequential CuAAC reactions on a [5:1]fullerene hexakis-adduct precursor bearing ten azide functional groups and two TMS-protected alkyne units, Iehl *et al.* prepared the fullerene based artificial light-harvesting arrays  $\text{Y}_{10}\text{B}_2\text{C}_{60}$  (Fig. 10) in excellent isolated yields with the objective to evaluate and characterize the energy transfer processes within polymer films doped with  $\text{Y}_{10}\text{B}_2\text{C}_{60}$ .<sup>87</sup> The advantage of this synthetic route is that it generates asymmetric fullerene derivatives bearing ten yellow and two blue boron dipyrromethene (Bodipy) dyes, thus displaying a gradient of energy levels around the  $\text{C}_{60}$  core that is known to exhibit only low absorption of visible light spectrum. The authors showed that in dry films, energy-transfer occurs such that photons absorbed by the yellow dyes are efficiently emitted by the blue dye. As a first proof of concept, a single layer PMMA-based luminescent solar concentrator (LSC) containing a low density of  $\text{Y}_{10}\text{B}_2\text{C}_{60}$  was built and used to sensitize usual amorphous silicon photocell. The obtained photocell was found to display an average light-to-electricity conversion of *ca.* 5% under ambient light conditions, proving that these decorated nanoparticles sensitize amorphous silicon photocells with increased absorption potential. The biggest challenge lies with self-assembling the loaded  $\text{C}_{60}$  particles into a loose network where inter-particle energy transfer is optimized.

Molecular switches and nanomachines have attracted considerable attention within the last years to build responsive materials for many applications. For instance, many efforts have been made to generate molecules in which electric stimulus results in molecular motions. Iehl *et al.* reported a copper-mediated Huisgen 1,3-dipolar cycloaddition starting from easily accessible fullerene hexakis-adduct **70** (1 equiv.) bearing twelve peripheral azide functional groups in the presence of  $97 \cdot 2\text{PF}_6$  (13 equiv.),  $\text{Cu}(\text{MeCN})_4\text{PF}_6$  (0.1 equiv.), and tris-[(1-benzyl-1*H*-1,2,3-triazol-4-yl)methyl]amine (0.1 equiv.) in DMF for 24 h at room temperature (Scheme 32).<sup>88</sup> Compound





**Scheme 31** Synthetic route to [5:1] fullerene hexakis-adduct.<sup>86</sup>

**98** was thus obtained in 78% yield. Viologens ( $V^{2+}$ ) are usually easily converted to radical cations  $V^{\bullet+}$  upon a one electron reduction process that further leads to  $\pi$ -dimerization at high concentrations of viologen units.

The authors evaluated this feature of the viologen terminal units within fullerene **98**, demonstrating that upon reduction, six intramolecular  $\pi$ -dimers are formed leading to fullerene molecules able to electrochemically and reversibly switch from an “open” charge-repelled state (twelve arms) to a “close” state (six arms). These multiple “open/close” molecular movements around the  $C_{60}$  core, triggered by electron-transfers centered on the  $\pi$ -dimerizable bipyridinium units, have been shown to occur in organic solvents and in aqueous media. This system opens the way towards more elaborate redox switchable structures where mechanically interlocked molecules could be incorporated around the all-carbon sphere using a similar synthetic protocol.

We have discussed the fact that the  $C_{60}$  core can be transformed to fullerene hexakis-adducts of  $C_{2v}$  symmetry by sequential Bingel reactions with two different malonates. Using this approach, Brettreich *et al.* prepared globular amphiphiles described in Scheme 33.<sup>89</sup> First, malonate **99** (obtained from malonyl dichloride and two equivalents of the corres-

ponding alcohol) was reacted with  $C_{60}$  in a nucleophilic Bingel cyclopropanation reaction to afford the expected monoadduct **100**. Next, the five remaining octahedral positions on  $C_{60}$  were functionalized in a DMA-templated cyclopropanation involving didodecyl malonate to give the expected mixed hexakis-adduct **101** in 23% isolated yield. *tert*-Butyl groups were then removed with TFA, unmasking the terminal carboxylic acids that were then reacted with amide dendron **102** in presence DCC and HOBT to give the intermediate in 30% yield. A final treatment of the latter product with TFA gave access to fullerene amphiphile **103** bearing 18 carboxylic acid groups on the hydrophilic tail and ten dodecyl chains in the hydrophobic region. Aggregation of **103** was studied by UV spectroscopy, TEM and light scattering measurements, showing that it forms spontaneously vesicles of approximately 100–400 nm, which is similar to those obtained from common phospholipids. However, it was observed that compounds **103** tend to form unilamellar aggregates, as well as a variety of different bilayered structures.

The influence of polyaddition of malonates to  $C_{60}$  was also explored with the intent of forming chiral liquid-crystalline phases and appeared to be a suitable approach to generate a wide variety of mesomorphic materials.<sup>90–92</sup>



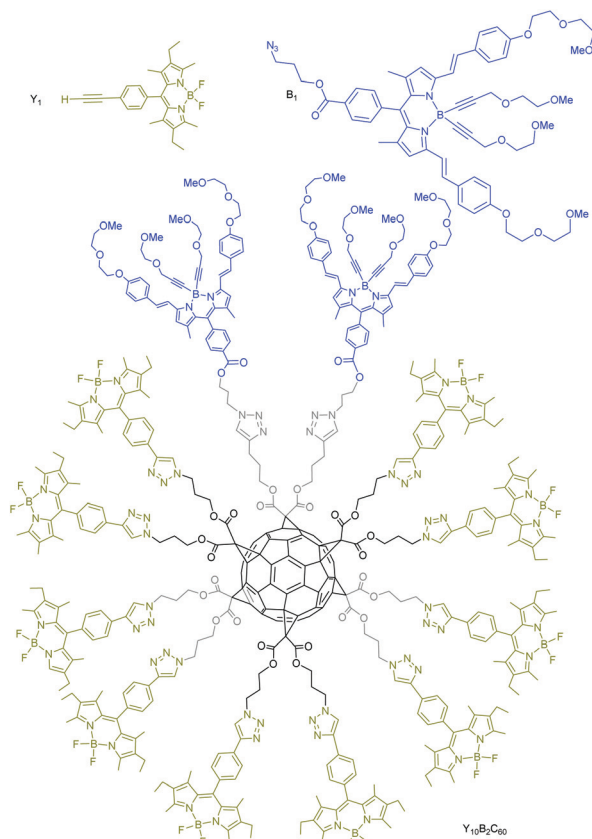
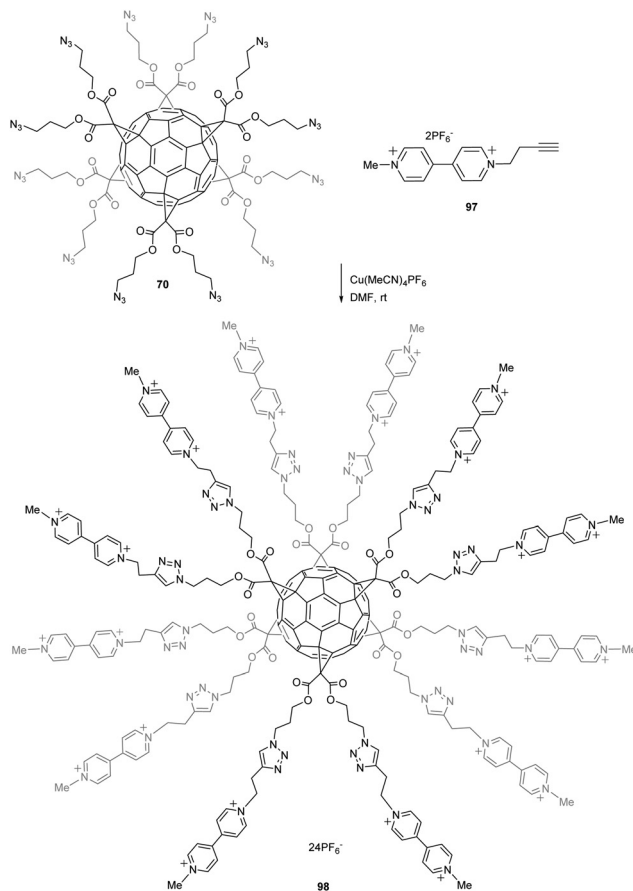
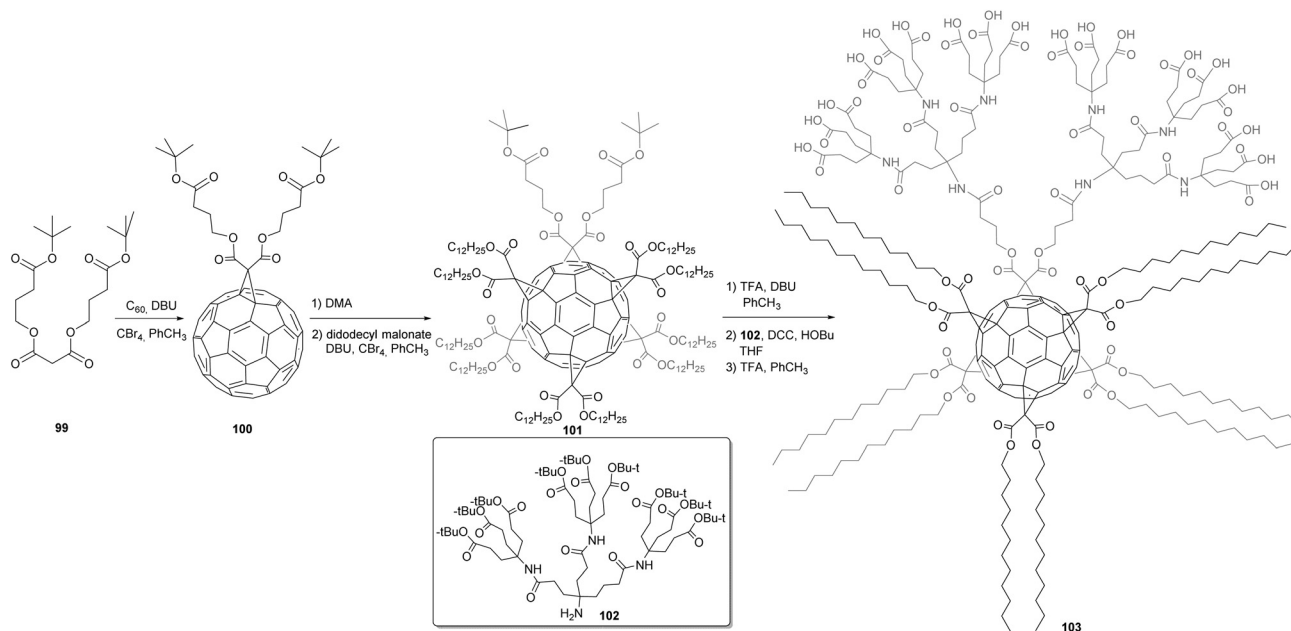


Fig. 10 Structure of C<sub>60</sub> hexakis-adduct Y<sub>10</sub>B<sub>2</sub>C<sub>60</sub> decorated with yellow and blue Bodipy-based dyes.



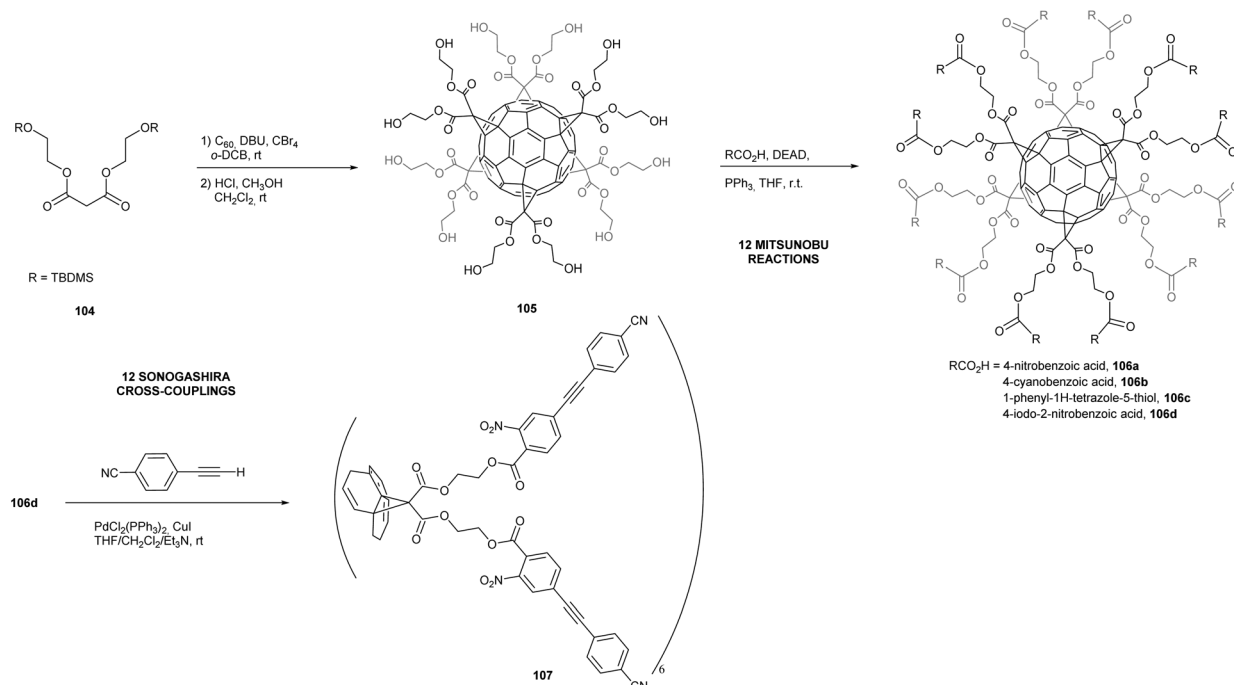
Scheme 32 Synthetic route to hexakis-adduct C<sub>60</sub> with viologen sub-units around the core.<sup>88</sup>



Scheme 33 Synthetic route to globular amphiphiles based on hexakis-adducts of C<sub>60</sub>.<sup>89</sup>

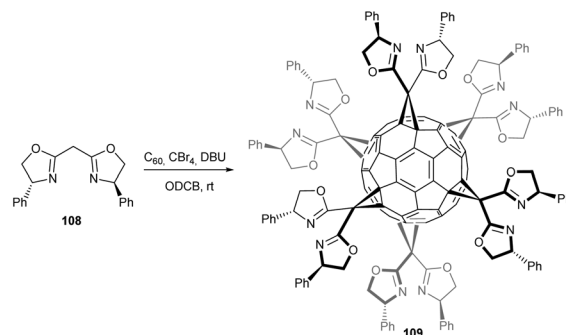






Scheme 34 Mitsunobu and Sonogashira cross-coupling reactions to post-functionalize fullerene hexakis-adducts.<sup>93</sup>

The direct introduction of six bulky malonates around the fullerene  $C_{60}$  through Bingel cyclopropanation reactions is rapidly slowed down by the large malonates, and results in the formation of the expected hexakis-adduct with low to negligible yield. To overcome this problem, several groups have developed methods for post-functionalization of the methanofullerene adducts. For instance, Nierengarten *et al.* adapted the copper-mediated Huisgen 1,3-dipolar cycloaddition reaction and applied it to the preparation of complex hexa-substituted fullerenes from a easily accessible dodecaazide derivative, as discussed before. Additionally, Pierrat *et al.* developed a synthetic strategy using a Mitsunobu post-functionalization of a hexa-substituted fullerene derivative bearing twelve hydroxyl groups (Scheme 34).<sup>93</sup> The silyl-protected malonate **104** was conjugated to  $C_{60}$  using usual Bingel conditions to form the expected hexakis-adduct that was further deprotected to give polyol **105** in 28% over two steps. The latter was then successfully functionalized by a Mitsunobu reaction in the presence of a range of activated carboxylic acids. The reaction was optimized with a combination of diethyl azodicarboxylate (DEAD) as oxidizing azo-reagent and triphenylphosphine (TPP) as reducing agent, which gave the desired dodeca-esters in moderate to good yields (Scheme 34). Moreover, the product **106d** bearing twelve aromatic iodide units was further transformed by efficient Sonogashira cross-coupling reactions to afford product **107** in 52% yield, that corresponds to 95% per iodide. Although results obtained so far suggest that this approach is limited to activated Mitsunobu substrates, this approach enables for third generation derivatization of the fullerene substrates.



Scheme 35 Synthetic route to enantiomerically pure novel [6:0]hexakis[(bisoxazoliny)methano]fullerenes.<sup>37</sup>

Seifermann *et al.* reported on the first enantiomerically pure [6:0]hexakis[(bisoxazoliny)methano]fullerene derivatives shown in Scheme 35, which were obtained *via* cyclopropanation of  $C_{60}$  with the corresponding  $C_2$ -symmetrical enantiomerically pure bis(oxazolines) **108** and adaptation of the conditions developed by the Sun group (100-fold excess  $CBr_4$ ).<sup>37</sup> In these conditions, both enantiomers of the phenyl derivatives *all-S*-**109** and *all-R*-**109** were obtained in 32% and 31% yield, respectively. These compounds provide an all-organic rigid scaffold bearing six orthogonally directed metal-chelation sites. Preliminary experiments indicate that the generation of six-fold metal-complexes is possible. Thus, this new material holds great promise in terms of potential applications in asymmetric catalysis as well as tectons for the



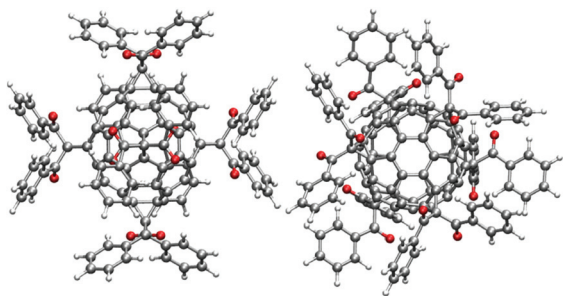
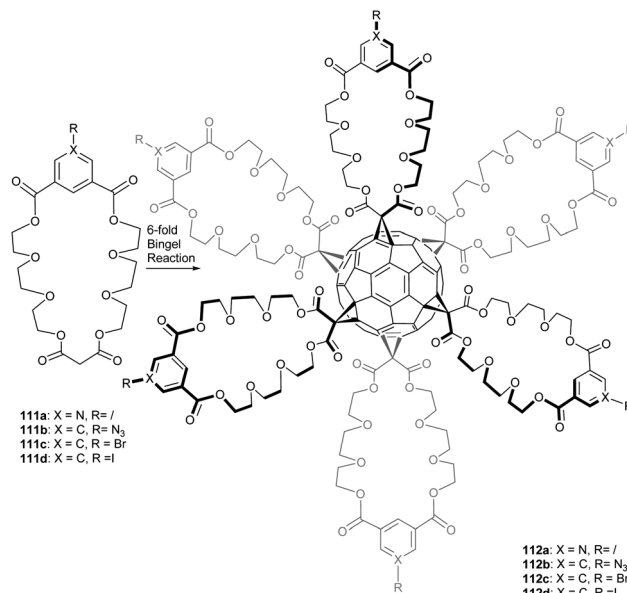


Fig. 11 Structure of hexakis-diphenylmethane adduct **110** based on DFT calculations.<sup>63</sup>

construction of enantiomerically pure supramolecular 3D structures.

Since the discovery of the Bingel reaction, malonates and  $\beta$ -keto esters are starting materials of choice to functionalize the fullerene core and to access various fullerene adducts. Recently, our group reported the synthesis of hexakis-diphenylmethane adduct that could have applications in the construction of 3D metal organic frameworks owing to the coordination properties of 1,3-diketones.<sup>63</sup> The reaction conditions involved the use of  $\alpha$ -bromo dibenzoylmethane (6 equiv.) with the non-nucleophilic base  $P(tBu)_3$  in toluene. After column chromatography, the expected product **110** (Fig. 11) was clearly identified by  $^1H$  NMR and MALDI-TOF-MS. Unfortunately, the title compound contained some aliphatic impurities that could not be removed by any purification methods tested so far.

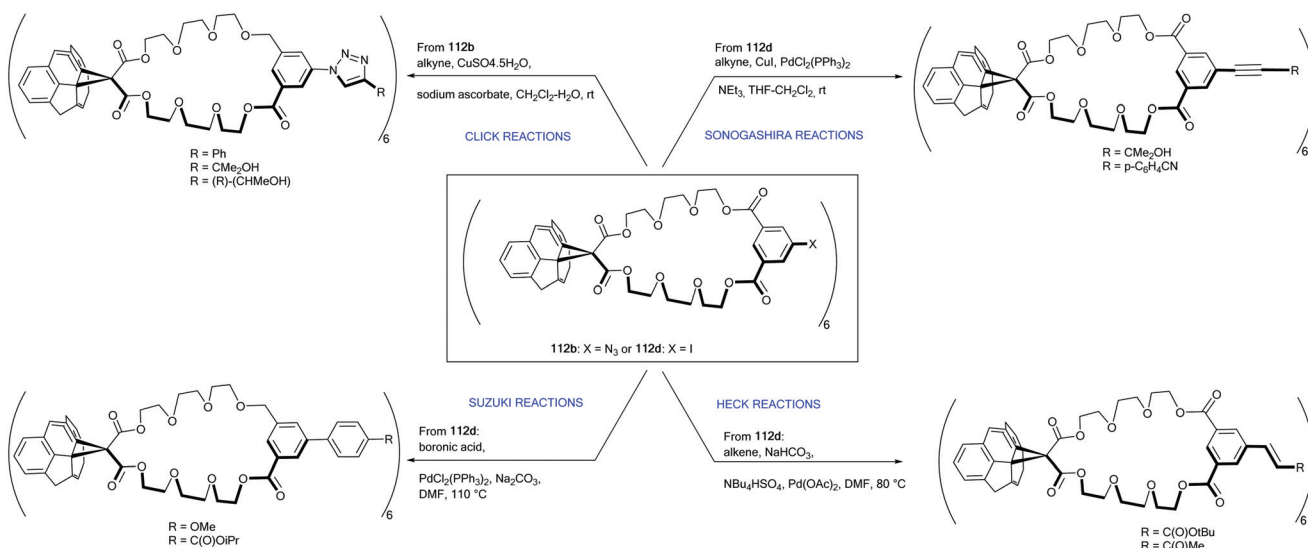
The method of choice to synthesize hexakis-methanofullerenes deals with the Bingel reaction involving malonates. This route leads to the formation of dodeca-substituted products with only limited applications as octahedral building blocks in material science. To circumvent this problem, Pierrat *et al.* reported on the synthesis of hexakis-substituted fullerene



Scheme 36 Synthetic access to hexakis-substituted fullerenes bearing six sticky sides.

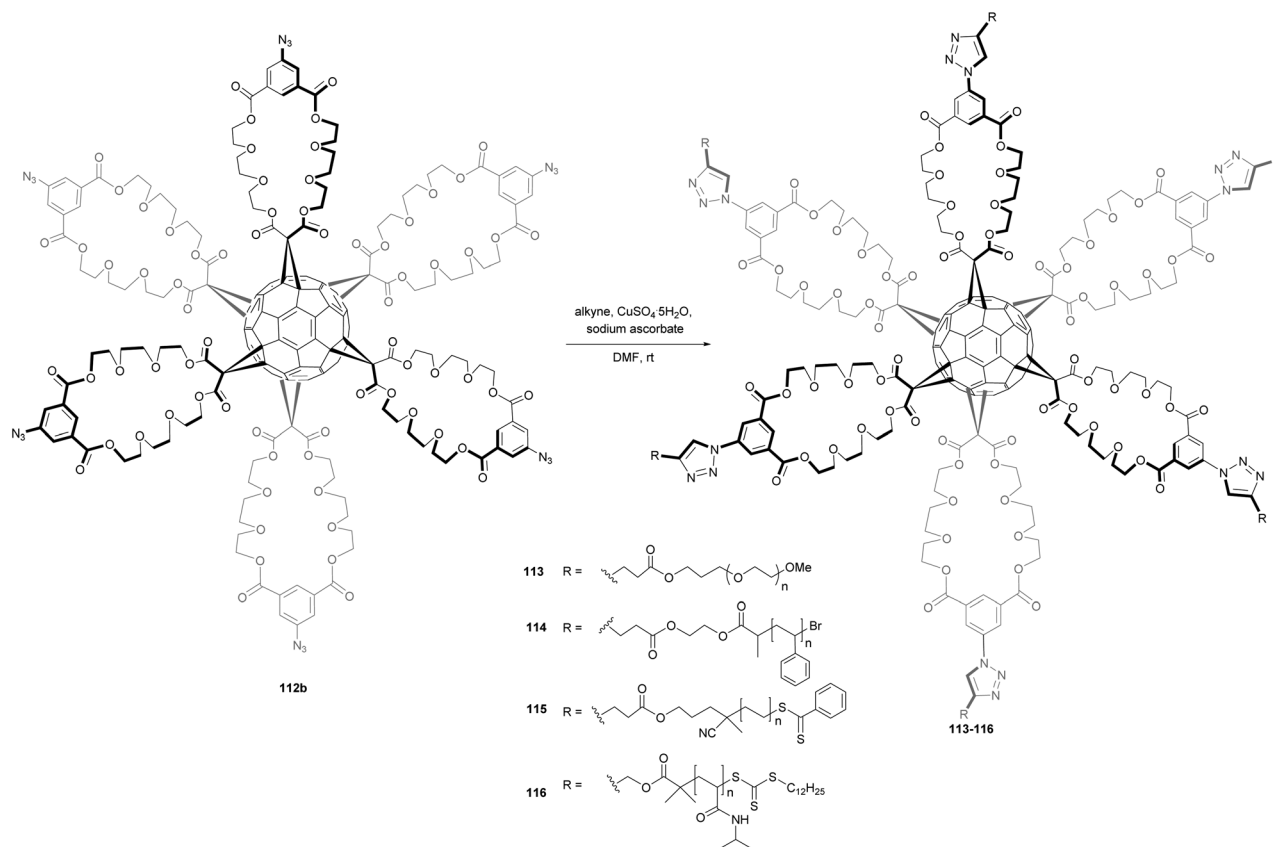
adducts **112a–d** bearing only six peripheral functional groups (halides, pyridine and azide) from the corresponding malonate-isophthalate oxyethylene macrocycles that were anchored onto the  $C_{60}$  by the usual Bingel reaction (Scheme 36).<sup>94</sup> Derivative **112a** bearing six peripheral pyridine sticky sides is a useful starting point to generate octahedral metal–organic frameworks through metal–ligand recognition processes.

Interestingly, compounds **112b** (bearing six peripheral azides) and **112c** (bearing six aromatic iodides) could be further functionalized by Click chemistry and various cross-coupling reactions (Scheme 37). The cross-coupling reactions presented are modular, tolerant to a wide range of functional



Scheme 37 Six-fold Huisgen, Sonogashira, Suzuki and Heck reactions on fullerene hexakis-adducts.





**Scheme 38** Synthetic route to star-shaped polymer-fullerene hybrids.

groups and high-yielding. This method easily opens synthetic access to a large number of functionalized  $T_h$  symmetric fullerene derivatives.

Using this synthetic approach, Inglis *et al.* reported the first examples of well-defined  $\text{C}_{60}$ -based star polymers, whose structures have been confirmed by gel permeation chromatography and  $^1\text{H}$  NMR spectroscopy.<sup>18</sup> These  $\text{C}_{60}$ -based star polymers were prepared by the CuAAC of alkyne-terminated polymers **113–116** with  $\text{C}_{60}\text{-N}_3$  in the presence of copper(II)sulfate and sodium ascorbate in DMF (Scheme 38). It was shown that compound **116**, bearing six peripheral poly(*n*-isopropylacrylamide) (PNIPAM) showed quick reversible, thermally-induced flocculation in water. This contribution has thus shown that hexakis-azido fullerene derivative **112b** may be efficiently used in the synthesis of well-defined, star-shaped polymers *via* click chemistry. The authors demonstrated that the use of a large, sterically non-demanding core such as  $\text{C}_{60}$  allows for a near flawless star construction even at high molecular weights. In addition, thermoresponsive star-shaped fullerene derivatives are easily accessible by this synthetic route.

MOFs containing  $\text{C}_{60}$  linkers in well-defined geometries would be expected to exhibit unique structures and properties.

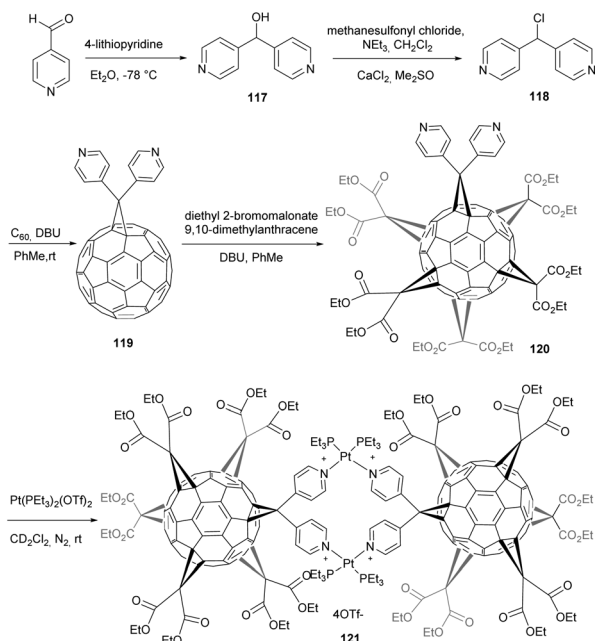
Habicher *et al.* reported on the synthesis and X-ray crystal structure of fullerene-containing rigid dinuclear cyclophane which was obtained by self-assembly of the novel fullerene ligand with Pt(II) centres.<sup>95</sup> Dipyridylchloromethane **118** was

treated under the usual Bingel cyclopropanation method to afford the fullerene monoadduct **119** in 32% yield (Scheme 39). Any attempt to form metal complexes from fullerene **119**, was unsuccessful because of the low solubility of the fullerene monoadduct.

In order to overcome this problem, the authors prepared the yellow  $\text{C}_{2v}$ -symmetrical fullerene hexakis-adduct **120** by DMA-templated addition of diethyl 2-bromomalonate on fullerene **119**. Next, by mixing an equimolar amount of fullerene hexakis-adduct and  $[\text{cis-Pt}(\text{PET}_3)_2(\text{OTf})_2]$  in  $\text{CD}_2\text{Cl}_2$  at room temperature, the tetracationic cyclophane **121** was obtained quantitatively as its tetrakis-triflate salt. The structure of the complex was fully characterized by means of NMR spectroscopy ( $^1\text{H}$ ,  $^{13}\text{C}$ ,  $^{19}\text{F}$  and  $^{31}\text{P}$ ) and by X-ray crystal structure analysis. This structure highlights the potential of metal-directed self-assembly to build complex supermolecular fullerene arrays. For instance, by replacing further diethyl malonate substituents with dipyridylmethano groups, larger assemblies such as rods or two- and three-dimensional fullerene networks were accessible.

Peng *et al.* reported the synthesis of a new fullerene linker and its use in the formation of a linear coordination polymer by silver complexation (Scheme 40).<sup>96</sup> A new hexakis-fullerene adduct with two 4,5-diazafluorene groups strategically located at *trans*-1 positions to allow linear polymerization was selectively synthesized in very high yield. A one dimensional



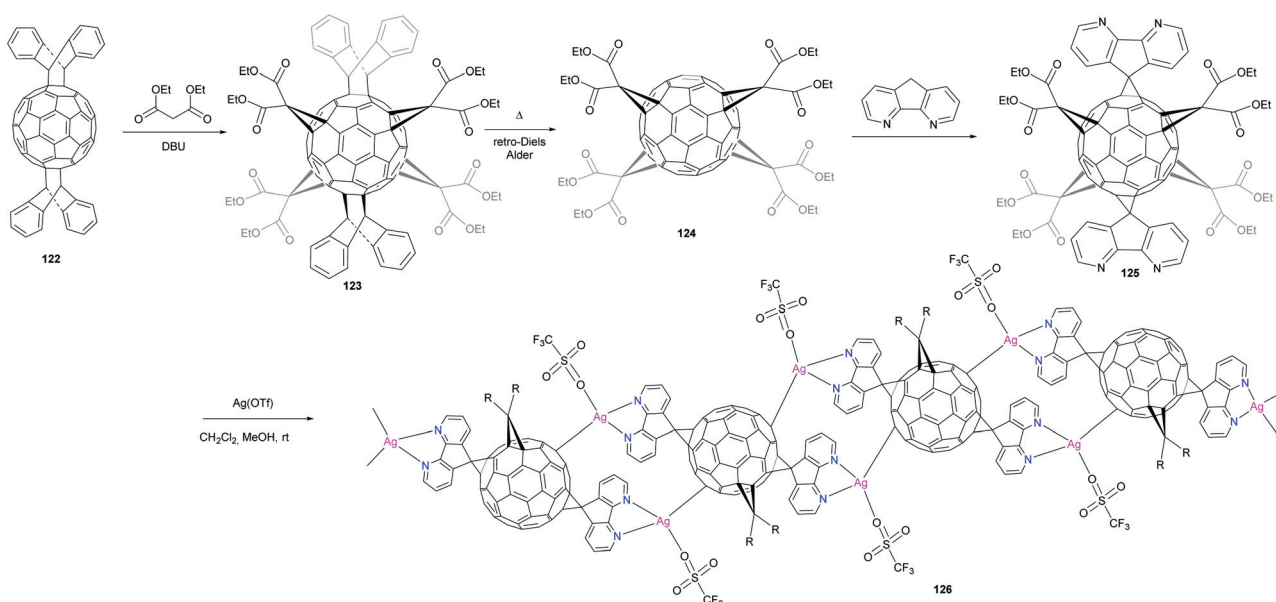


**Scheme 39** Synthetic route to a Pt(II)-central dinuclear cyclophane-containing two fullerene units.

metal-organic coordination polymer was obtained by reaction with silver triflate. The 4,5-diazafluorene group was selected since it can efficiently react in the Bingel method and is known to be an excellent ligand for metal coordination. The synthesis of mono-unit **125** for coordination was accomplished starting with the bis-adduct of  $C_{60}$  with anthracene protecting groups located in the *trans* positions. The remaining four equatorial positions around the  $C_{60}$  were then decorated by symmetric addition of four diethyl malonate groups. The anthracene groups were removed by a heat-mediated retro-

Diels–Alder reaction to afford tetrakis-functional fullerene **124**, which was subsequently reacted with 4,5-diazafluorene to produce the hexakis-*trans*-1 adduct **125** in 91% yield. Light yellow-green crystals of the polymeric silver complex were obtained by slow diffusion of silver triflate in methanol into a solution of mono-unit **125** solubilized in dichloromethane followed by the addition of toluene. The structure of the crystal was characterized by X-ray crystal structure analysis. No intermolecular interactions between fullerene units were observed. This was explained by the presence of four bulky equatorial ethyl malonate groups on the  $C_{60}$  cage. Interestingly, diazafluorene rings of adjacent fullerenes interact clearly by  $\pi$ – $\pi$  interactions. Furthermore, the coordination geometry of the silver centre can be considered as distorted tetrahedral. Thus, hexakis-substituted fullerene adducts with coordination sites are suitable building blocks for the generation of linear polymers through coordination with metal ions.

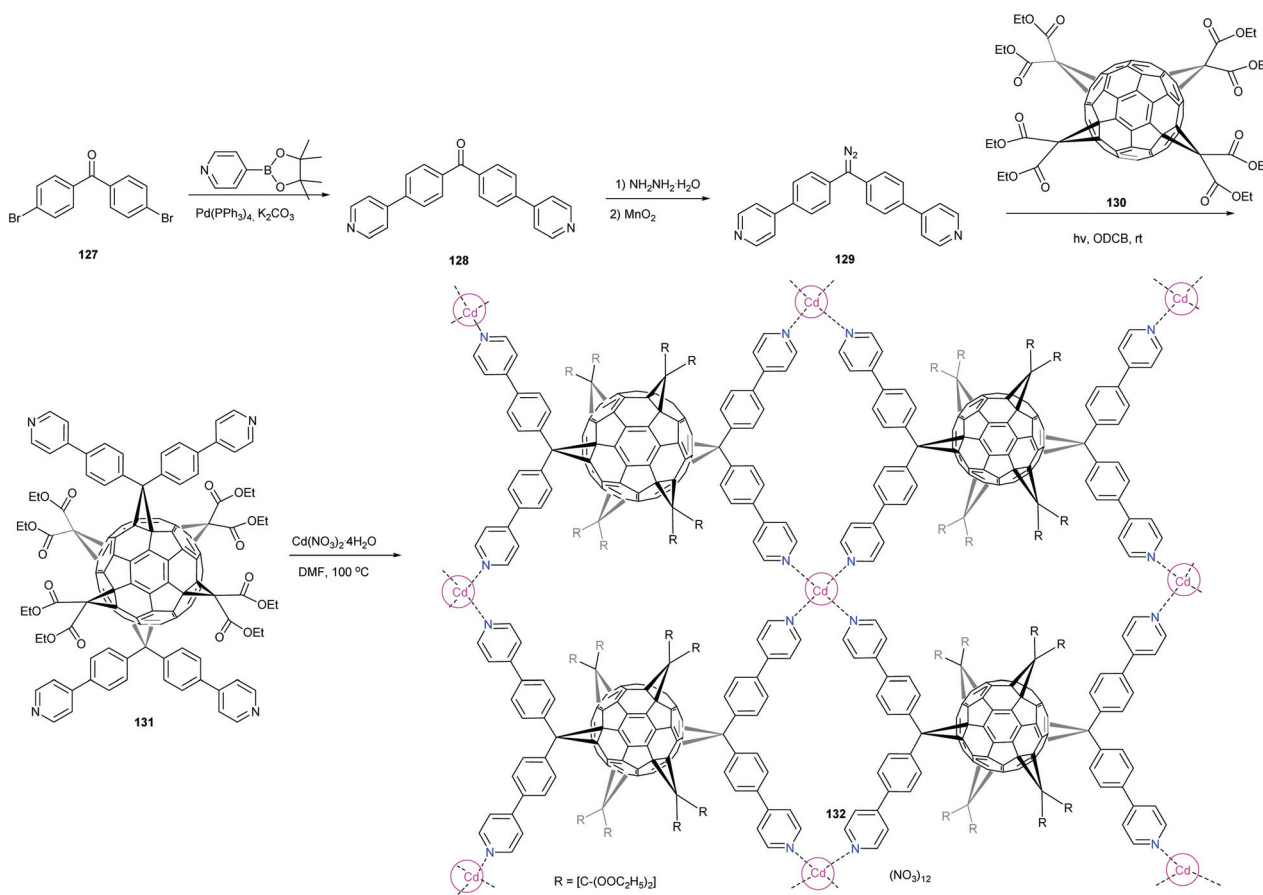
Recently, Peng *et al.* reported the design and synthesis of a hexakisfullerene adduct with four pyridyl groups whose nitrogen atoms reside in a rectangle.<sup>14</sup> This adduct was employed as a linker to build the first two-dimensional (2D) fullerene-based MOF. The 2D layers packed in the crystal with interlayers composed of isolated hexakisfullerene molecules form an intricate three-dimensional (3D) structure (Scheme 41). The authors used tetrakis[di(ethoxycarbonyl)methano]- $C_{60}$  **130** as a starting material and reacted it under photoirradiation at 365 nm with 4,4'-(4,4'-(diazomethylene)bis(4,1-phenylene))-dipyridine **129** to access the hexakis-adduct **131**, which displayed a  $D_{2h}$  symmetry according to  $^1\text{H}$  NMR spectroscopy. Compound **131** was designed to have four pyridyl nitrogen atoms, to define a perfectly planar rectangle. Crystals of complex **131**[(**130**)<sub>2</sub>·Cd(NO<sub>3</sub>)<sub>2</sub>]<sub>∞</sub> were obtained by the reaction of **5** with Cd(NO<sub>3</sub>)<sub>2</sub>·4H<sub>2</sub>O in DMF at 100 °C, followed by careful addition of methanol to the cooled solution. Single-crystal



**Scheme 40** Synthetic route to a new fullerene linker and linear silver-coordination polymer.







**Scheme 41** Synthetic route to the first fullerene-linked 2D metal-organic framework.

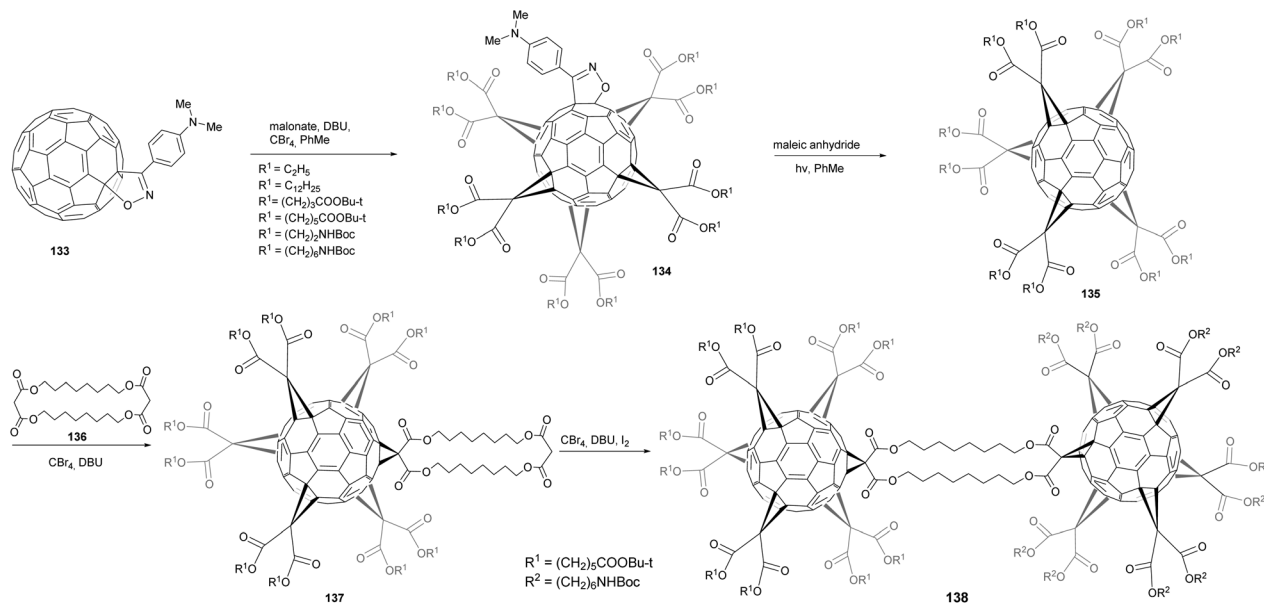
X-ray diffraction analysis clearly showed the single layer formed upon coordination of **131** with cadmium cations, in which each pyridine group coordinates with four different cadmium ions. Furthermore, the fullerene pillars exhibit interactions with the layers surrounding them. On the basis of these results, it is anticipated that by connecting metal centres of the 2D fullerene layers with dipyrindine-based pillars, 3D MOF can be built.

Hörmann *et al.* have reported the preparation of  $C_{2v}$ -symmetrical pentakis-adducts of  $C_{60}$  as versatile building blocks for fullerene architectures that involve a mixed octahedral addition pattern.<sup>97</sup> To efficiently synthesize such structures, the authors developed a strategy involving isoxazolinofullerenes **133** (Scheme 42) in which the isoxazoline moiety can be considered a protecting group as it can be easily removed by efficient retro-cycloaddition by refluxing in *o*-dichlorobenzene in the presence of an excess of a dienophile. Fullerene **133** was subjected to five-fold cyclopropanation at octahedral positions in the presence of  $CBr_4$ , DBU and a range of malonates to afford the expected product **134** in 29–53% yields. The completion of the octahedral addition pattern was accomplished by means of five-fold cyclopropanation with malonate and  $CBr_4$  in the presence of DBU. Deprotection of the protected [5:1]hexakis-adducts was achieved under irradiation and in the

presence of maleic anhydride in 44–79% yields. Cyclopropanation of **135** with cyclic bismalonate **136** afforded adduct **137** in 86% yield, that could be further functionalized in the presence of **135**,  $CBr_4$  and DBU to give **136** in 67% yield. Thus, the authors have introduced a new protection-deprotection sequence for the selective and efficient synthesis of a variety of  $C_{2v}$ -symmetrical fullerene pentakis-adducts with an incomplete octahedral addition pattern. Through the use of this protecting group, the hexakis-adduct synthesis that often represents the yield-limiting step, was done at the beginning of the synthesis, which reduced the quantities of malonate needed and made the purification process easier.

Moreover, the use of  $C_{2v}$ -symmetrical fullerene pentakis-adducts **135** for the synthesis of [5:1]hexakis-adducts afforded a convergent synthesis. The isoxazoline protection-deprotection strategy was successfully applied to the synthesis of a heptakis-fullerene **139** (Fig. 12).<sup>98</sup> The success of this synthesis relied on the mono-activation of the bis-malonate cyclo[2]-octylmalonate **140** (Scheme 43). The authors demonstrated that the introduction of a bromide atom is not suitable for this purpose due to unexpected scrambling of the bromide atom between both malonate sides in the presence of DBU. This was not observed with a chloride atom at this position. Nevertheless, it was shown that chlorinated malonates are less reactive





Scheme 42 Synthetic route to  $\text{C}_{2v}$ -symmetrical pentakis-adducts of  $\text{C}_{60}$  to synthesize [5:1]hexakis-adducts.

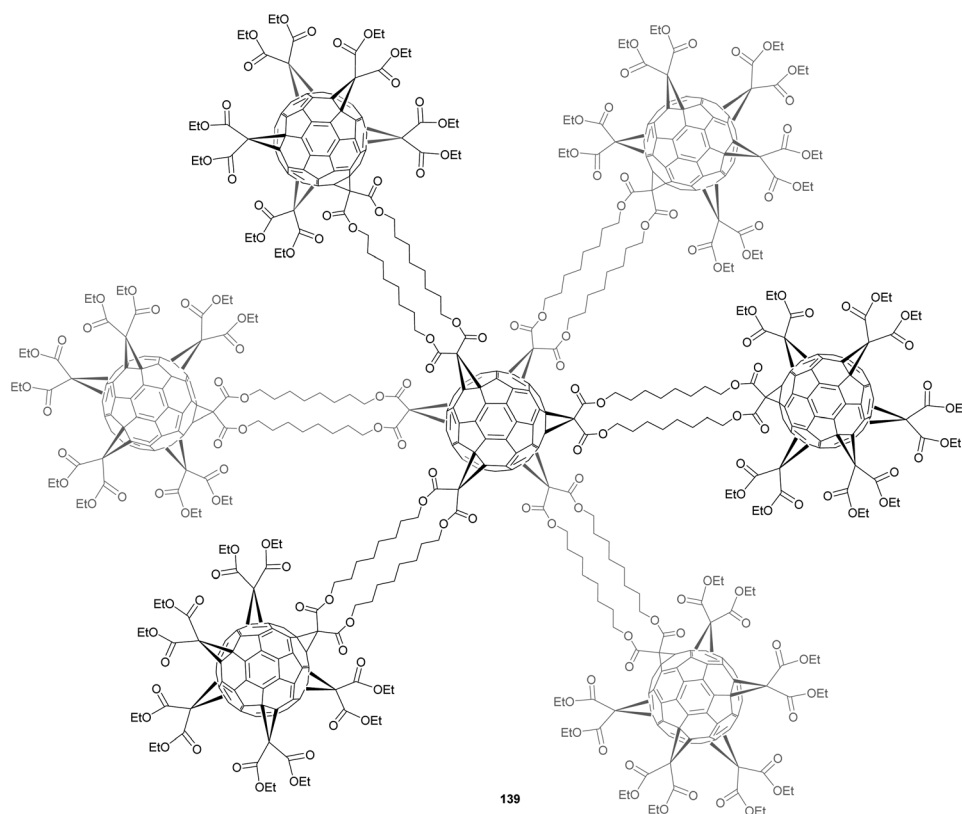
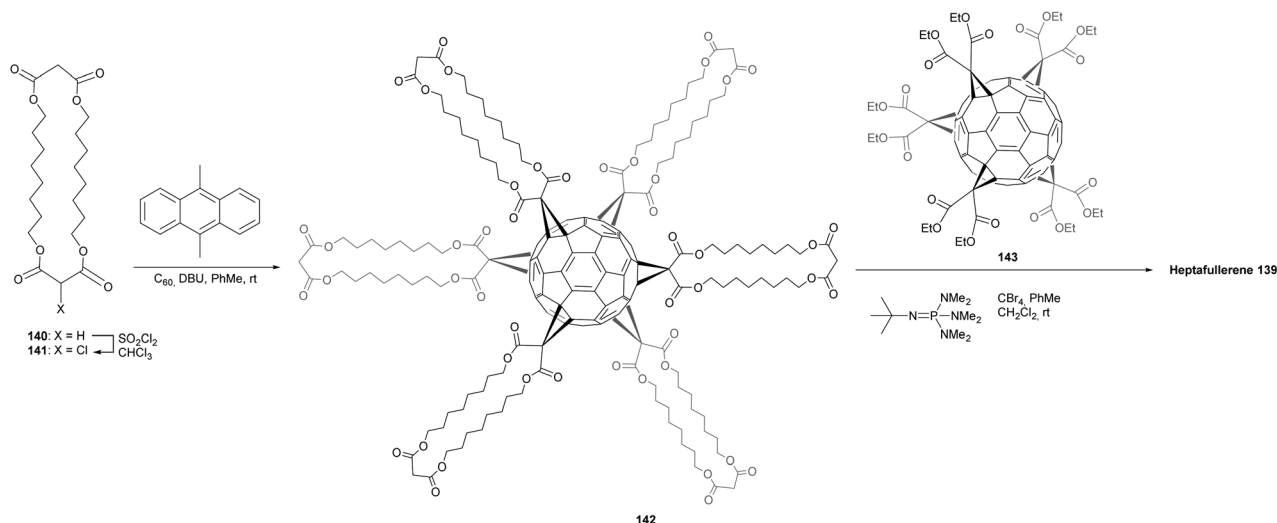


Fig. 12 Structure of the heptaful fullerene 139.

than the brominated ones for the substitution of  $\text{C}_{60}$  in the Bingel reaction. The monochlorination of **140** was performed in the presence of a stoichiometric amount of suluryl chloride to give the expected compound **141** in 36% isolated yield.

A 25-fold excess of substituents **141** was reacted with  $\text{C}_{60}$  by templating with 9,10-dimethylantracene to get the  $T_h$ -symmetric hexakis-adduct with DBU as a base in toluene as solvent. After purification by silica gel column chromato-





**Scheme 43** Synthetic route to oligocluster heptafullerene.

graphy, the expected hexakis-adduct **142** was isolated in 3.3% yield. In the final step, pentakis-substituted fullerene **143** (7 equiv.) prepared as described previously was conjugated to hexakis-adduct **142** in toluene in the presence of  $\text{CBr}_4$  and *tert*-butylimino-tri(pyrrolidino)phosphorane as a base.<sup>97</sup> Owing to solubility problems, the reaction was stirred for one month at room temperature, and the expected heptafullerene was obtained after purification in 43% yield. Authors have thus developed an efficient approach for the sequential fullerenylation of bis-malonates with different fullerene units. This method for the sequential and orthogonal oligofunctionalization of oligomalonates bears many possibilities for the design of highly functional oligofullerene architectures with tunable properties.

## 2.6. Heptakis-substituted fullerenes

There are only a few reports dealing with the synthesis of hepta-substituted fullerenes. Most of them were synthesized by diazomethane addition and characterized by mass-spectroscopy.<sup>99–104</sup> As there no structural details corroborated by X-ray crystallography are known, these systems were not further discussed.

## 2.7. Octakis-substituted fullerenes

Octakis-substituted fullerenes are quite rare and were only produced by dipolar cycloaddition reactions.<sup>99</sup> As for these no structural details are known, structures are not shown herein.

## 2.8. Higher substituted fullerenes

Highly reactive species also lead to higher-substituted fullerenes. Some of them, such as octakis(trifluoromethyl)-octakishydrido fullerene were characterized by X-ray crystallography.<sup>105,106</sup>

## 3. Conclusions

It is remarkable that different  $\text{C}_{60}$ -derivatives can be obtained by controlling the accessible extent of functionalization of  $\text{C}_{60}$ . Most functionalized fullerenes described in this review were obtained in good to excellent yields and provide a number of useful and unique fullerene-based materials such as indene- $\text{C}_{60}$  bis-adduct and silylmethyl[60]fullerene for high-performance solar cells; self-assembly films; penta-haptofullerene metal complexes; liquid crystals, glycosidase inhibition with fullerene iminosugar balls; bacterial anti-adhesives, gene delivery with polycationic fullerene; artificial light-harvesting arrays; star shaped polymer-fullerene hybrids; fullerene-linked metal-organic frameworks. Some derivatives hold the promise of a number of applications; however, the application of these derivatives has not been deeply studied.

Given the number of developed methods to synthesize flexible structures, we anticipate that the key challenge is the construction of defined nanostructures according to specific needs in functional fullerene materials and biologically useful molecules, and so on. And it is anticipated this will be extensively investigated in the near future.

## Acknowledgements

We appreciate the stimulating atmosphere of the KIT fullerene group (mentioned in the publications) and also the reviewers for very useful comments. Our own work has been supported by the DFG (CFN).

## Notes and references

- 1 C. Thilgen and F. Diederich, *Chem. Rev.*, 2006, **106**, 5049–5135.



- 2 F. Giacalone and N. Martin, *Chem. Rev.*, 2006, **106**, 5136–5190.
- 3 O. Vostrowsky and A. Hirsch, *Chem. Rev.*, 2006, **106**, 5191–5207.
- 4 Y. Matsuo and E. Nakamura, *Chem. Rev.*, 2008, **108**, 3016–3028.
- 5 P. A. Troshin, A. S. Peregodov, S. I. Troyanov and R. N. Lyubovskaya, *Russ. Chem. Bull.*, 2008, **57**, 887–912.
- 6 U. Hahn, F. Vögtle and J. F. Nierengarten, *Polymers*, 2012, **4**, 501–538.
- 7 M. Prato, *J. Mater. Chem.*, 1997, **7**, 1097–1109.
- 8 S. S. Babu, H. Mohwald and T. Nakanishi, *Chem. Soc. Rev.*, 2010, **39**, 4021–4035.
- 9 P. Compain, C. Decroocq, J. Iehl, M. Holler, D. Hazelard, T. M. Barragan, C. O. Mellet and J. F. Nierengarten, *Angew. Chem., Int. Ed.*, 2010, **49**, 5753–5756.
- 10 M. Durka, K. Buffet, J. Iehl, M. Holler, J. F. Nierengarten, J. Taganna, J. Bouckaert and S. P. Vincent, *Chem. Commun.*, 2011, **47**, 1321–1323.
- 11 D. Sigwalt, M. Holler, J. Iehl, J. F. Nierengarten, M. Nothisen, E. Morin and J. S. Remy, *Chem. Commun.*, 2011, **47**, 4640–4642.
- 12 S. Cecioni, V. Oerthel, J. Iehl, M. Holler, D. Goyard, J. P. Praly, A. Imbert, J. F. Nierengarten and S. Vidal, *Chem. – Eur. J.*, 2011, **17**, 3252–3261.
- 13 Y. J. He, H. Y. Chen, J. H. Hou and Y. F. Li, *J. Am. Chem. Soc.*, 2010, **132**, 1377–1382.
- 14 P. Peng, F. F. Li, V. S. P. K. Neti, A. J. Metta-Magana and L. Echegoyen, *Angew. Chem., Int. Ed.*, 2014, **53**, 160–163.
- 15 T. M. Figueira-Duarte, J. Clifford, V. Amendola, A. Gegout, J. Olivier, F. Cardinal, M. Meneghetti, N. Armaroli and J. F. Nierengarten, *Chem. Commun.*, 2006, 2054–2056.
- 16 V. Garg, G. Kodis, M. Chachisvilis, M. Hambourger, A. L. Moore, T. A. Moore and D. Gust, *J. Am. Chem. Soc.*, 2011, **133**, 2944–2954.
- 17 M. Sawamura, K. Kawai, Y. Matsuo, K. Kanie, T. Kato and E. Nakamura, *Nature*, 2002, **419**, 702–705.
- 18 A. J. Inglis, P. Pierrat, T. Muller, S. Bräse and C. Barner-Kowollik, *Soft Matter*, 2010, **6**, 82–84.
- 19 M. G. Nava, S. Setayesh, A. Rameau, P. Masson and J. F. Nierengarten, *New J. Chem.*, 2002, **26**, 1584–589.
- 20 C. Bingel, *Chem. Ber./Recl.*, 1993, **126**, 1957–1959.
- 21 M. Prato, T. Suzuki, H. Foroudian, Q. Li, K. Khemani, F. Wudl, J. Leonetti, R. D. Little, T. White, B. Rickborn, S. Yamago and E. Nakamura, *J. Am. Chem. Soc.*, 1993, **115**, 1594–1595.
- 22 M. Prato, Q. C. Li, F. Wudl and V. Lucchini, *J. Am. Chem. Soc.*, 1993, **115**, 1148–1150.
- 23 T. Tago, T. Minowa, Y. Okada and J. Nishimura, *Tetrahedron Lett.*, 1993, **34**, 8461–8464.
- 24 H. H. Wang, J. A. Schlueter, A. C. Cooper, J. L. Smart, M. E. Whitten, U. Geiser, K. D. Carlson, J. M. Williams, U. Welp, J. D. Dudek and M. A. Caleca, *J. Phys. Chem. Solids*, 1993, **54**, 1655–1666.
- 25 P. Belik, A. Gugel, A. Kraus, J. Spickermann, V. Enkelmann, G. Frank and K. Mullen, *Adv. Mater.*, 1993, **5**, 854–856.
- 26 V. M. Rotello, J. B. Howard, T. Yadav, M. M. Conn, E. Viani, L. M. Giovane and A. L. Lafleur, *Tetrahedron Lett.*, 1993, **34**, 1561–1562.
- 27 F. Diederich, U. Jonas, V. Gramlich, A. Herrmann, H. Ringsdorf and C. Thilgen, *Helv. Chim. Acta*, 1993, **76**, 2445–2453.
- 28 B. Krautler and M. Puchberger, *Helv. Chim. Acta*, 1993, **76**, 1626–1631.
- 29 D. Babic, D. J. Klein and C. H. Sah, *Chem. Phys. Lett.*, 1993, **211**, 235–241.
- 30 F. Cardullo, P. Seiler, L. Isaacs, J. F. Nierengarten, R. F. Haldimann, F. Diederich, T. Mordasini-Denti, W. Thiel, C. Boudon, J. P. Gisselbrecht and M. Gross, *Helv. Chim. Acta*, 1997, **80**, 343–371.
- 31 T. Kusukawa and W. Ando, *Angew. Chem., Int. Ed. Engl.*, 1996, **35**, 1315–1317.
- 32 F. Cardullo, P. Seiler, L. Isaacs, J. F. Nierengarten, R. F. Haldimann, F. Diederich, T. Mordasini-Denti, W. Thiel, C. Boudon, J. P. Gisselbrecht and M. Gross, *Helv. Chim. Acta*, 1997, **80**, 343–371.
- 33 F. Hormann, M. Brettreich, W. Donaubaue, F. Hampel and A. Hirsch, *Chem. – Eur. J.*, 2013, **19**, 2814–2825.
- 34 M. Sawamura, H. Iikura and E. Nakamura, *J. Am. Chem. Soc.*, 1996, **118**, 12850–12851.
- 35 C. R. Woods, J. P. Bourgeois, P. Seiler and F. Diederich, *Angew. Chem., Int. Ed.*, 2000, **39**, 3813–3816.
- 36 I. Lamparth, C. Maichle-Mössmer and A. Hirsch, *Angew. Chem., Int. Ed. Engl.*, 1995, **34**, 1607–1609.
- 37 S. M. Seifermann, C. Rethore, T. Muller and S. Bräse, *Sci. Rep.*, 2013, **3**, 2817.
- 38 P. Seiler, L. Isaacs and F. Diederich, *Helv. Chim. Acta*, 1996, **79**, 1047–1058.
- 39 Y. Z. Tan, Z. J. Liao, Z. Z. Qian, R. T. Chen, X. Wu, H. Liang, X. Han, F. Zhu, S. J. Zhou, Z. P. Zheng, X. Lu, S. Y. Xie, R. B. Huang and L. S. Zheng, *Nat. Mater.*, 2008, **7**, 790–794.
- 40 T. M. Figueira-Duarte, V. Lloveras, J. Vidal-Gancedo, B. Delavaux-Nicot, C. Duhayon, J. Veciana, C. Rovira and J. F. Nierengarten, *Eur. J. Org. Chem.*, 2009, 5779–5787.
- 41 D. Sigwalt, M. Holler and J. F. Nierengarten, *Tetrahedron Lett.*, 2013, **54**, 3160–3163.
- 42 J.-F. Nierengarten, V. Gramlich, F. Cardullo and F. Diederich, *Angew. Chem., Int. Ed. Engl.*, 1996, **35**, 2101–2103.
- 43 Y. Matsuo, A. Iwashita, Y. Abe, C. Z. Li, K. Matsuo, M. Hashiguchi and E. Nakamura, *J. Am. Chem. Soc.*, 2008, **130**, 15429–15436.
- 44 Y. Matsuo, Y. Sato, T. Niinomi, I. Soga, H. Tanaka and E. Nakamura, *J. Am. Chem. Soc.*, 2009, **131**, 16048–16050.
- 45 F. Cardinali, J. L. Gallani, S. Schergna, M. Maggini and J. F. Nierengarten, *Tetrahedron Lett.*, 2005, **46**, 2969–2972.





- 46 J. Nierengarten, in *Dendrimers V*, ed. C. Schalley and F. Vögtle, Springer, Berlin, Heidelberg, 2003, vol. 228, ch. 4, pp. 87–110.
- 47 A. Hirsch and O. Vostrowsky, in *Dendrimers IV*, ed. F. Vögtle and C. Schalley, Springer, Berlin, Heidelberg, 2001, vol. 217, ch. 2, pp. 51–93.
- 48 J.-F. Nierengarten, *Chem. – Eur. J.*, 2000, **6**, 3667–3670.
- 49 R. van de Coevering, R. Kreiter, F. Cardinali, G. van Koten, J. F. Nierengarten and R. J. M. K. Gebbink, *Tetrahedron Lett.*, 2005, **46**, 3353–3356.
- 50 U. Hahn, E. Maisonhaute, C. Amatore and J. F. Nierengarten, *Angew. Chem., Int. Ed.*, 2007, **46**, 951–954.
- 51 A. Hirsch, I. Lamparth and H. R. Karfunkel, *Angew. Chem., Int. Ed. Engl.*, 1994, **33**, 437–438.
- 52 D. Sigwalt, F. Schillinger, S. Guerra, M. Holler, M. Berville and J. F. Nierengarten, *Tetrahedron Lett.*, 2013, **54**, 4241–4244.
- 53 F. Beuerle and A. Hirsch, *Chem. – Eur. J.*, 2009, **15**, 7447–7455.
- 54 S. Guerra, F. Schillinger, D. Sigwalt, M. Holler and J. F. Nierengarten, *Chem. Commun.*, 2013, **49**, 4752–4754.
- 55 L. Isaacs, F. Diederich and R. F. Haldimann, *Helv. Chim. Acta*, 1997, **80**, 317–342.
- 56 C. Thilgen, S. Sergeev and F. Diederich, *Top. Curr. Chem.*, 2004, **248**, 1–61.
- 57 J. F. Nierengarten, T. Habicher, R. Kessinger, F. Cardullo, F. Diederich, V. Gramlich, J. P. Gisselbrecht, C. Boudon and M. Gross, *Helv. Chim. Acta*, 1997, **80**, 2238–2276.
- 58 F. Djojo and A. Hirsch, *Chem. – Eur. J.*, 1998, **4**, 344–356.
- 59 F. Djojo, A. Hirsch and S. Grimme, *Eur. J. Org. Chem.*, 1999, 3027–3039.
- 60 I. Lamparth and A. Hirsch, *J. Chem. Soc., Chem. Commun.*, 1994, 1727–1728.
- 61 T. B. Cao, F. Wei, Y. L. Yang, L. Huang, X. S. Zhao and W. X. Cao, *Langmuir*, 2002, **18**, 5186–5189.
- 62 H. Li, S. A. Haque, A. Kitaygorodskiy, M. J. Meziani, M. Torres-Castillo and Y.-P. Sun, *Org. Lett.*, 2006, **8**, 5641–5643.
- 63 A. Giovannitti, S. M. Seifermann, A. Bihlmeier, T. Muller, F. Topic, K. Rissanen, M. Nieger, W. Kloppe and S. Bräse, *Eur. J. Org. Chem.*, 2013, **2013**, 7907–7913.
- 64 Y. Murata, M. Shiro and K. Komatsu, *J. Am. Chem. Soc.*, 1997, **119**, 8117–8118.
- 65 Y. Matsuo, A. Muramatsu, R. Hamasaki, N. Mizoshita, T. Kato and E. Nakamura, *J. Am. Chem. Soc.*, 2004, **126**, 432–433.
- 66 M. Sawamura, Y. Kuninobu, M. Toganoh, Y. Matsuo, M. Yamanaka and E. Nakamura, *J. Am. Chem. Soc.*, 2002, **124**, 9354–9355.
- 67 Y. Matsuo, H. Isobe, T. Tanaka, Y. Murata, M. Murata, K. Komatsu and E. Nakamura, *J. Am. Chem. Soc.*, 2005, **127**, 17148–17149.
- 68 F. Wang, Z. Xiao, Z. Yao, Z. Jia, S. Huang, L. Gan, J. Zhou, G. Yuan and S. Zhang, *J. Org. Chem.*, 2006, **71**, 4374–4382.
- 69 J. Shiea, J.-P. Huang, C.-F. Teng, J. Jeng, L. Y. Wang and L. Y. Chiang, *Anal. Chem.*, 2003, **75**, 3587–3595.
- 70 S. C. Chueh, M. K. Lai, M. S. Lee, L. Y. Chiang, T. I. Ho and S. C. Chen, *Transplant. Proc.*, 1999, **31**, 1976–1977.
- 71 H. Li, Y. Li, J. Zhai, G. Cui, H. Liu, S. Xiao, Y. Liu, F. Lu, L. Jiang and D. Zhu, *Chem. – Eur. J.*, 2003, **9**, 6031–6038.
- 72 H. Li, Y. Zhou, Y. Li, Y. Song, H. Fang, S. Xiao, H. Liu, H. Gan, T. Jiu and D. Zhu, *Chem. Phys. Lett.*, 2004, **383**, 230–234.
- 73 P. J. Fagan, J. C. Calabrese and B. Malone, *J. Am. Chem. Soc.*, 1991, **113**, 9408–9409.
- 74 B. Kräutler and J. Maynollo, *Angew. Chem., Int. Ed. Engl.*, 1995, **34**, 87–88.
- 75 G. Schick, M. Levitus, L. Kvetko, B. A. Johnson, I. Lamparth, R. Lunkwitz, B. Ma, S. I. Khan, M. A. Garcia-Garibay and Y. Rubin, *J. Am. Chem. Soc.*, 1999, **121**, 3246–3247.
- 76 A. Hirsch, I. Lamparth, T. Groesser and H. R. Karfunkel, *J. Am. Chem. Soc.*, 1994, **116**, 9385–9386.
- 77 L. Isaacs, R. F. Haldimann and F. Diederich, *Angew. Chem., Int. Ed. Engl.*, 1994, **33**, 2339–2342.
- 78 X. Camps and A. Hirsch, *J. Chem. Soc., Perkin Trans. 1*, 1997, 1595–1596.
- 79 H. Li, A. Kitaygorodskiy, R. A. Carino and Y.-P. Sun, *Org. Lett.*, 2005, **7**, 859–861.
- 80 J. Iehl, R. P. de Freitas, B. Delavaux-Nicot and J. F. Nierengarten, *Chem. Commun.*, 2008, 2450–2452.
- 81 J. Iehl and J. F. Nierengarten, *Chem. – Eur. J.*, 2009, **15**, 7306–7309.
- 82 J. F. Nierengarten, J. Iehl, V. Oerthel, M. Holler, B. M. Illescas, A. Munoz, N. Martin, J. Rojo, M. Sanchez-Navarro, S. Cecioni, S. Vidal, K. Buffet, M. Durka and S. P. Vincent, *Chem. Commun.*, 2010, **46**, 3860–3862.
- 83 I. Nierengarten, K. Buffet, M. Holler, S. P. Vincent and J.-F. Nierengarten, *Tetrahedron Lett.*, 2013, **54**, 2398–2402.
- 84 R. Risquez-Cuadro, J. M. Garcia Fernandez, J.-F. Nierengarten and C. Ortiz Mellet, *Chem. – Eur. J.*, 2013, **19**, 16791–16803.
- 85 I. Nierengarten and J.-F. Nierengarten, *Chem. – Asian J.*, 2014, **9**, 1436–1444.
- 86 P. Fortgang, E. Maisonhaute, C. Amatore, B. Delavaux-Nicot, J. Iehl and J. F. Nierengarten, *Angew. Chem., Int. Ed.*, 2011, **50**, 2364–2367.
- 87 J. Iehl, J. F. Nierengarten, A. Harriman, T. Bura and R. Ziessel, *J. Am. Chem. Soc.*, 2012, **134**, 988–998.
- 88 J. Iehl, M. Frascioni, H. P. J. de Rouville, N. Renaud, S. M. Dyar, N. L. Strutt, R. Carmieli, M. R. Wasielewski, M. A. Ratner, J. F. Nierengarten and J. F. Stoddart, *Chem. Sci.*, 2013, **4**, 1462–1469.
- 89 M. Brettreich, S. Burghardt, C. Bottcher, T. Bayerl, S. Bayerl and A. Hirsch, *Angew. Chem., Int. Ed.*, 2000, **39**, 1845–1848.
- 90 T. Chuard, R. Deschenaux, A. Hirsch and H. Schonberger, *Chem. Commun.*, 1999, 2103–2104.



- 91 S. Campidelli, T. Brandmueller, A. Hirsch, I. M. Saez, J. W. Goodby and R. Deschenaux, *Chem. Commun.*, 2006, 4282–4284.
- 92 S. Gottis, C. Kopp, E. Allard and R. Deschenaux, *Helv. Chim. Acta*, 2007, **90**, 957–962.
- 93 P. Pierrat, C. Rethore, T. Muller and S. Bräse, *Chem. – Eur. J.*, 2009, **15**, 11458–11460.
- 94 P. Pierrat, S. Vanderheiden, T. Muller and S. Bräse, *Chem. Commun.*, 2009, 1748–1750.
- 95 T. Habicher, J. F. Nierengarten, V. Gramlich and F. Diederich, *Angew. Chem., Int. Ed.*, 1998, **37**, 1916–1919.
- 96 P. Peng, F. F. Li, F. L. Bowles, V. S. P. K. Neti, A. J. Metta-Magana, M. M. Olmstead, A. L. Balch and L. Echegoyen, *Chem. Commun.*, 2013, **49**, 3209–3211.
- 97 F. Hörmann, W. Donaubaue, F. Hampel and A. Hirsch, *Chem. – Eur. J.*, 2012, **18**, 3329–3337.
- 98 L. K. Wasserthal, A. Kratzer and A. Hirsch, *Eur. J. Org. Chem.*, 2013, 2355–2361.
- 99 R. F. Haldimann, F. G. Klarner and F. Diederich, *Chem. Commun.*, 1997, 237–238.
- 100 A. Herrmann, M. W. Ruttimann, T. Gibtnier, C. Thilgen, F. Diederich, T. Mordasini and W. Thiel, *Helv. Chim. Acta*, 1999, **82**, 261–289.
- 101 J. P. Bourgeois, C. R. Woods, F. Cardullo, T. Habicher, J. F. Nierengarten, R. Gehrig and F. Diederich, *Helv. Chim. Acta*, 2001, **84**, 1207–1226.
- 102 R. F. Haldimann, C. Fokas and F. Diederich, *Helv. Chim. Acta*, 2001, **84**, 1635–1660.
- 103 M. J. van Eis, P. Seiler, L. A. Muslinkina, M. Badertscher, E. Pretsch, F. Diederich, R. J. Alvarado, L. Echegoyen and I. P. Nunez, *Helv. Chim. Acta*, 2002, **85**, 2009–2055.
- 104 Y. Chen, Y. L. Wang, A. Rassat, P. Sinay, Y. Zhao and Y. M. Zhang, *Tetrahedron*, 2006, **62**, 2045–2049.
- 105 I. E. Kareev, N. B. Shustova, B. S. Newell, S. M. Miller, O. P. Anderson, S. H. Strauss and O. V. Boltalina, *Acta Crystallogr., Sect. E: Struct. Rep. Online*, 2006, **62**, O3154–O3156.
- 106 N. B. Shustova, D. V. Peryshkov, I. E. Kareev, O. V. Boltalina and S. H. Strauss, *Acta Crystallogr., Sect. E: Struct. Rep. Online*, 2007, **63**, O3398–U2441.

